Carbon Nanotubes: Electronic Properties and Devices

10/27/2005

Metallic vs. semiconducting nanotubes

n_1-n_2=3q,
one of the slices crosses K_1, metallic nanotubes

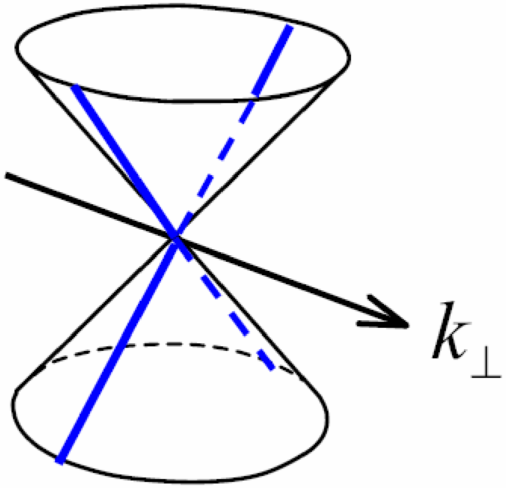

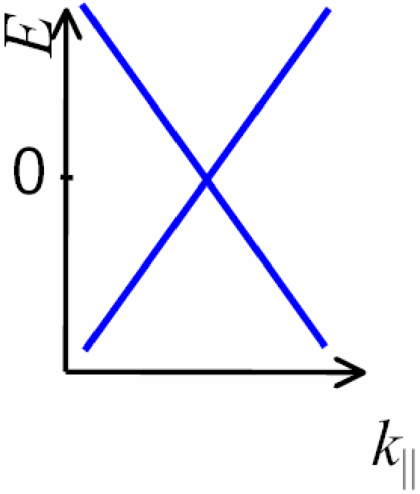

(armchair tubes (n_1=n_2) are metallic)

n_1-n_2≠3q,
No slice crosses K_1, semiconducting nanotubes

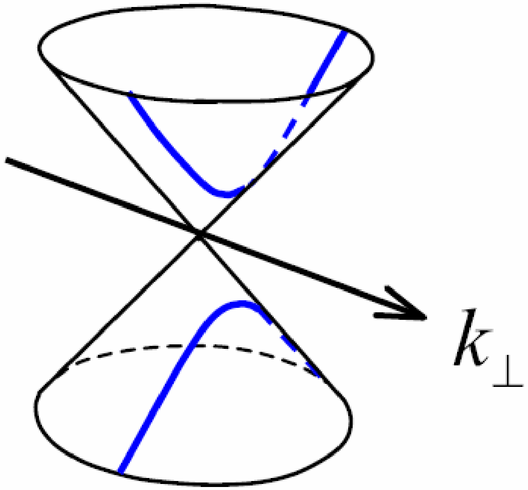

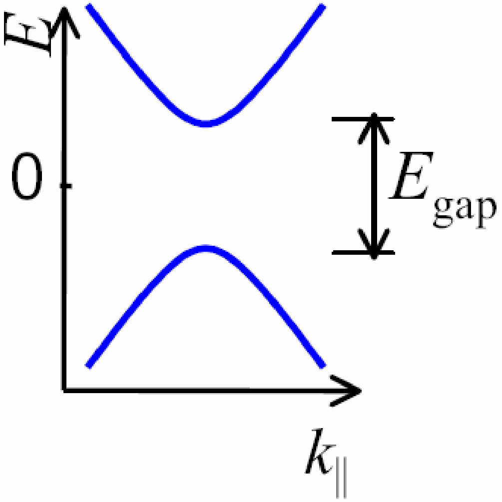

E_g~0.7eV/D (nm)

Metallic carbon nanotubes, with large (tunnel) contact resistances

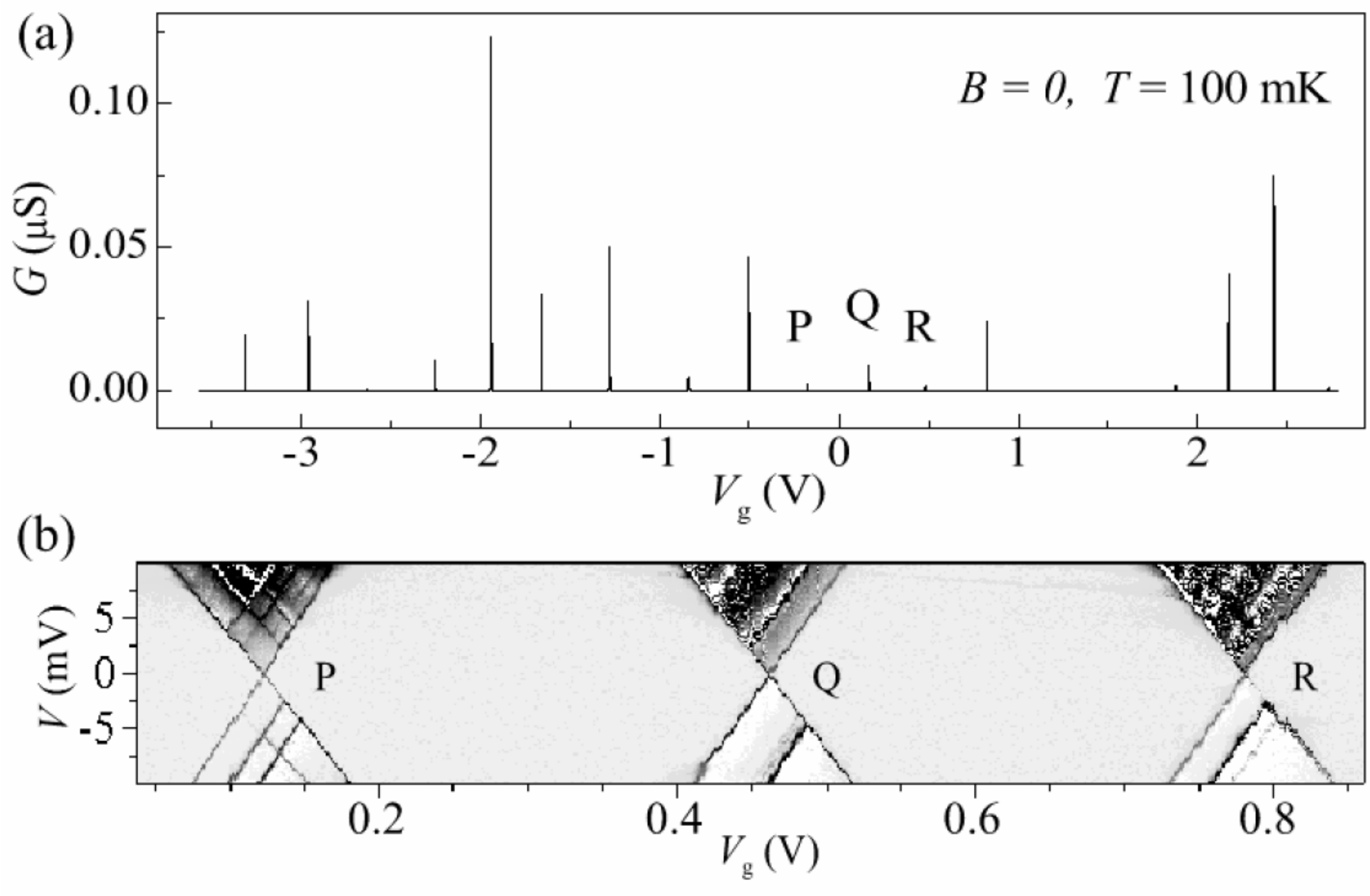

Nygard, Appl Phys. A. **69**, 297 (1999)

Metallic carbon nanotubes, with large (tunnel) contact resistances

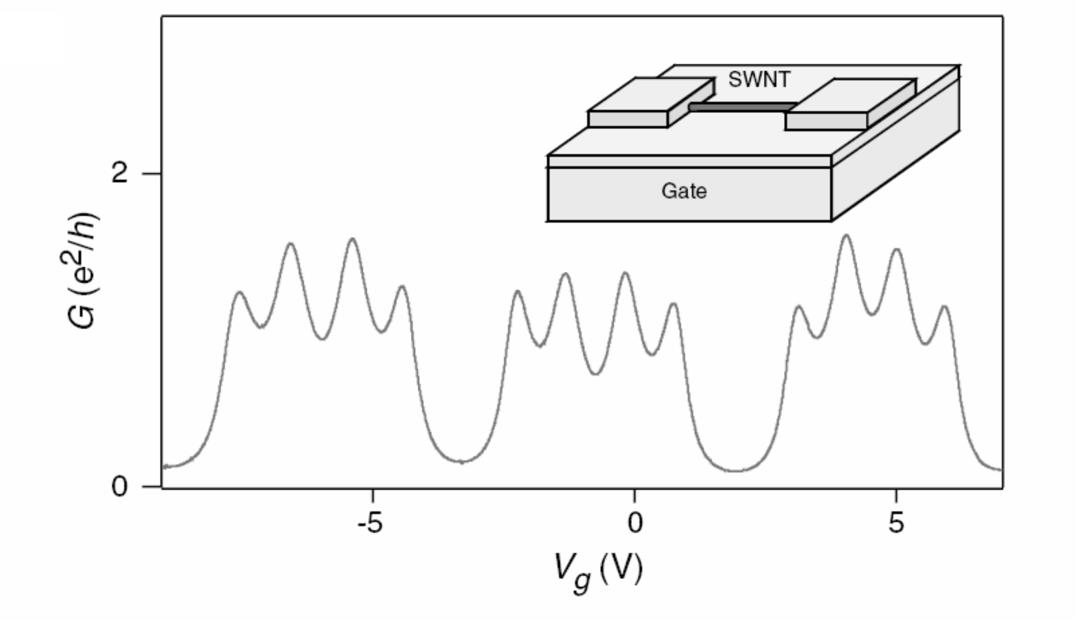

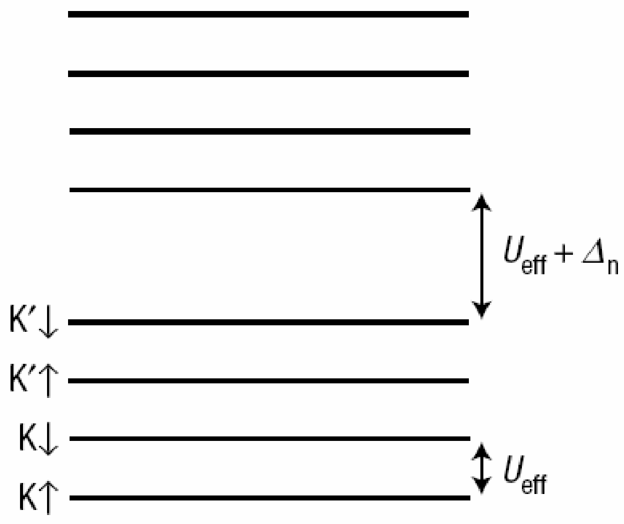

4-fold degeneracy. (2 by spin, 2 by orbital bands)

Liang, PRL, **88**, 126801, (2002)

Metallic carbon nanotubes, with small contact resistances

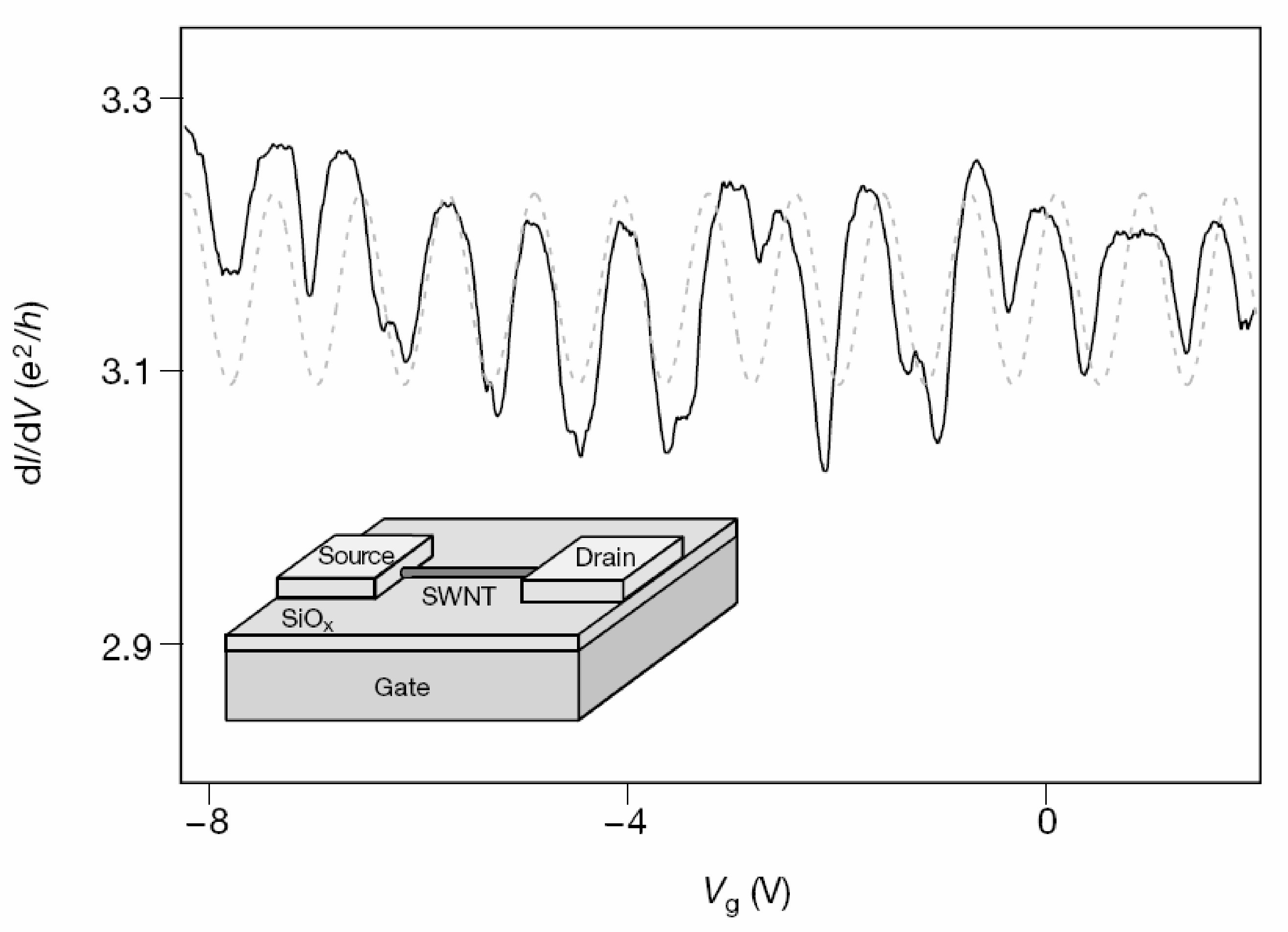

Ideal case: G=4e^2/h

Liang, Nature, **411**, 665 (2001)

Febry-Perot electro-interferometer

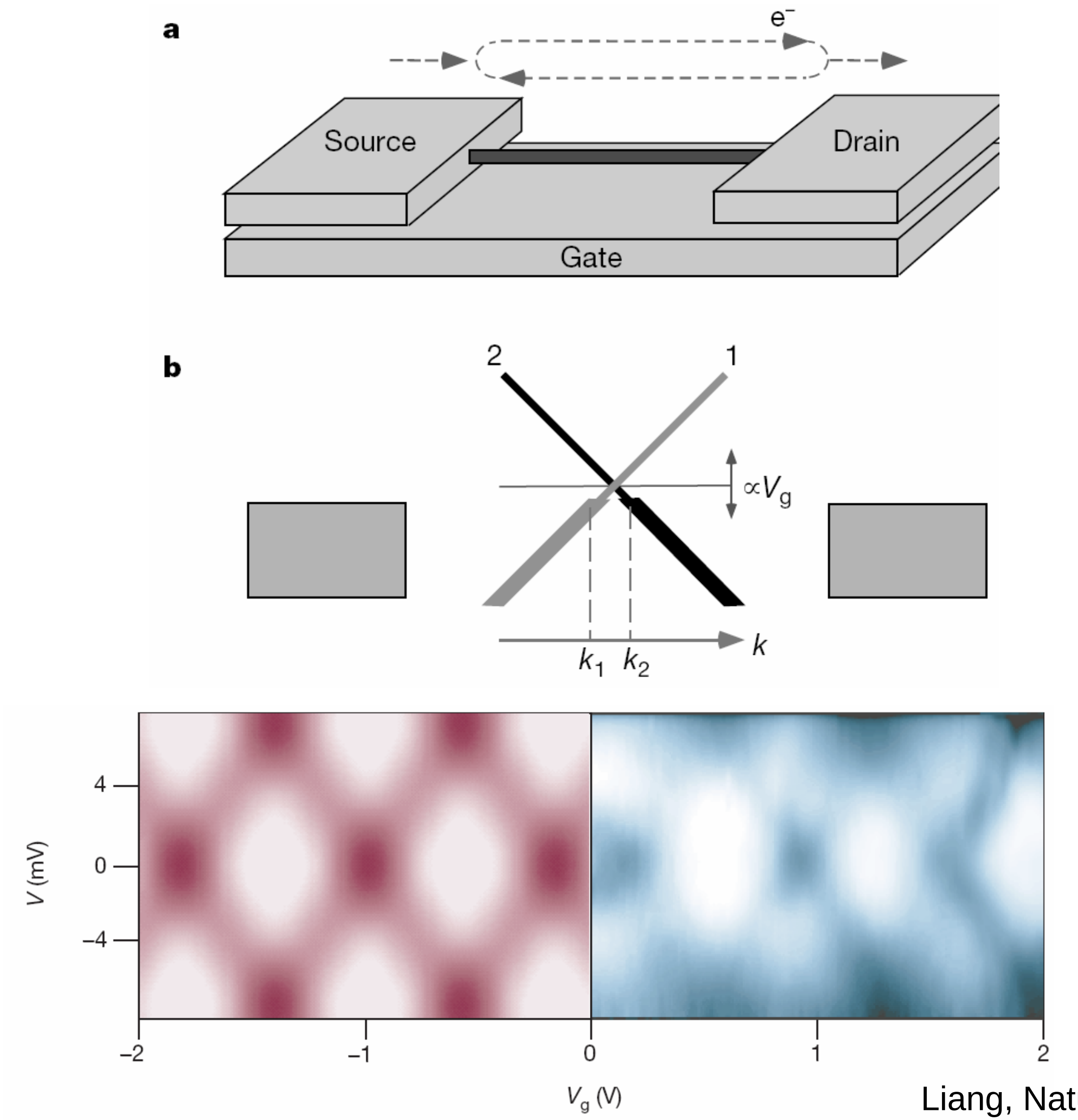

Liang, Nature, **411**, 665 (2001)

Febry-Perot electro-interferometer

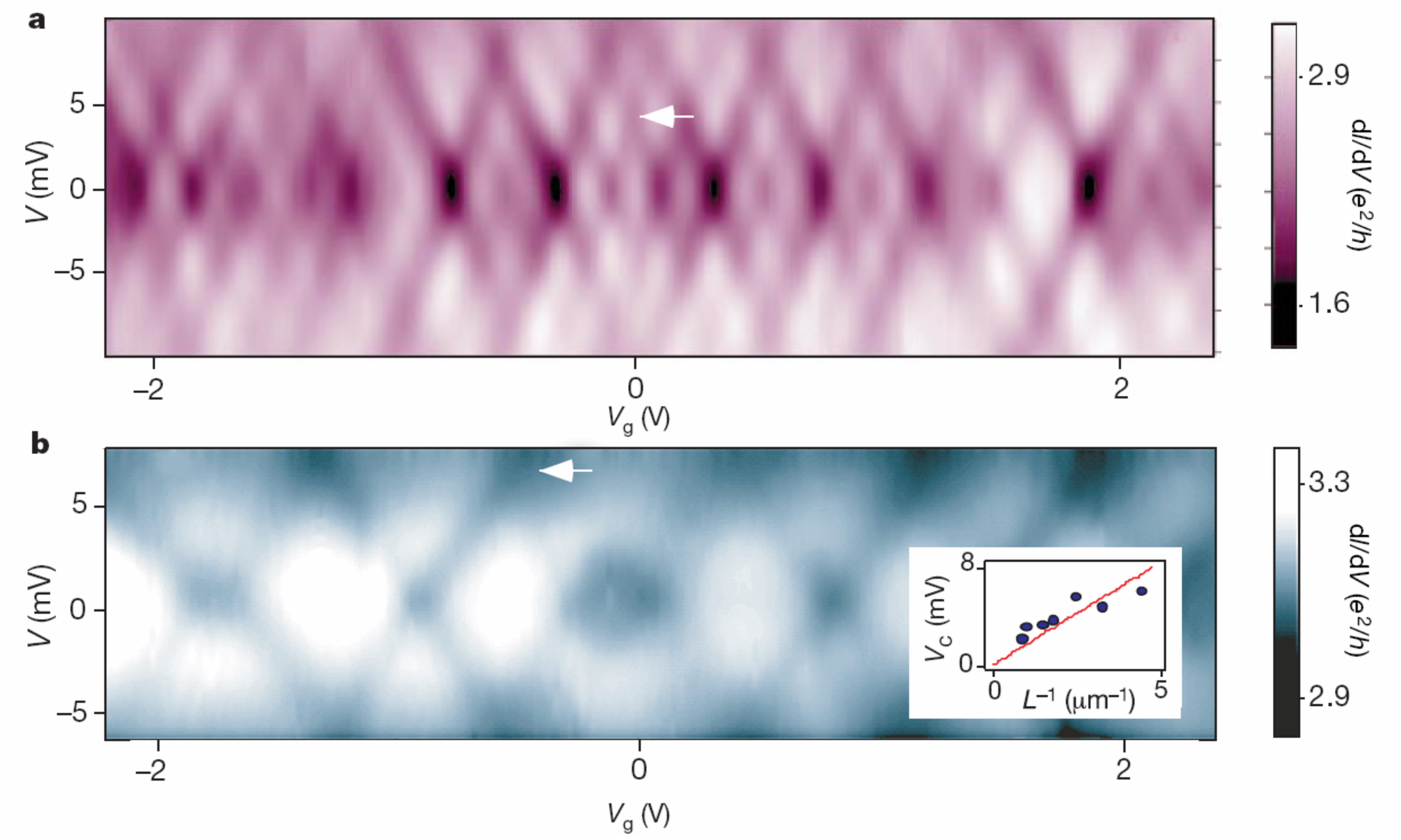

Liang, Nature, **411**, 665 (2001)

Room T, metallic tube

Park, Nano Lett, **4**, 517 (2004)

3 probe set-up

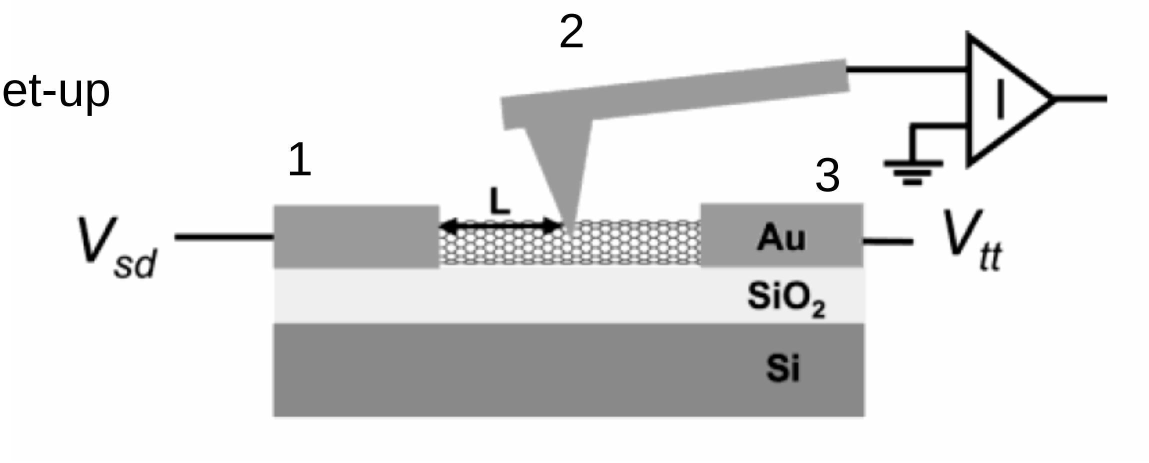

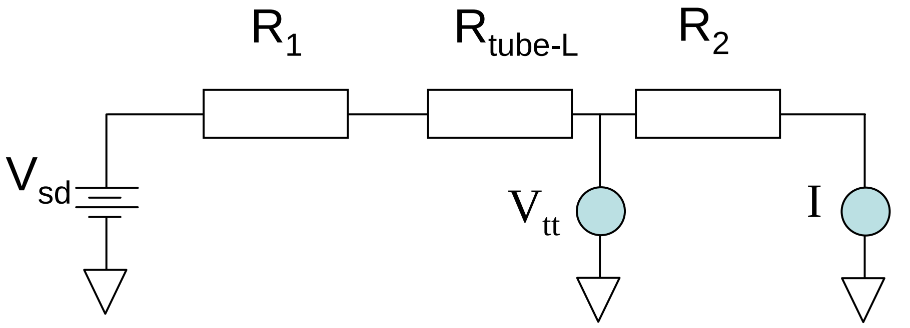

$V=V_{sd}-V_{tt}$

$V/I=R_1+R_{tube\text{-}L}$, independent of R_2

Room T, metallic tube

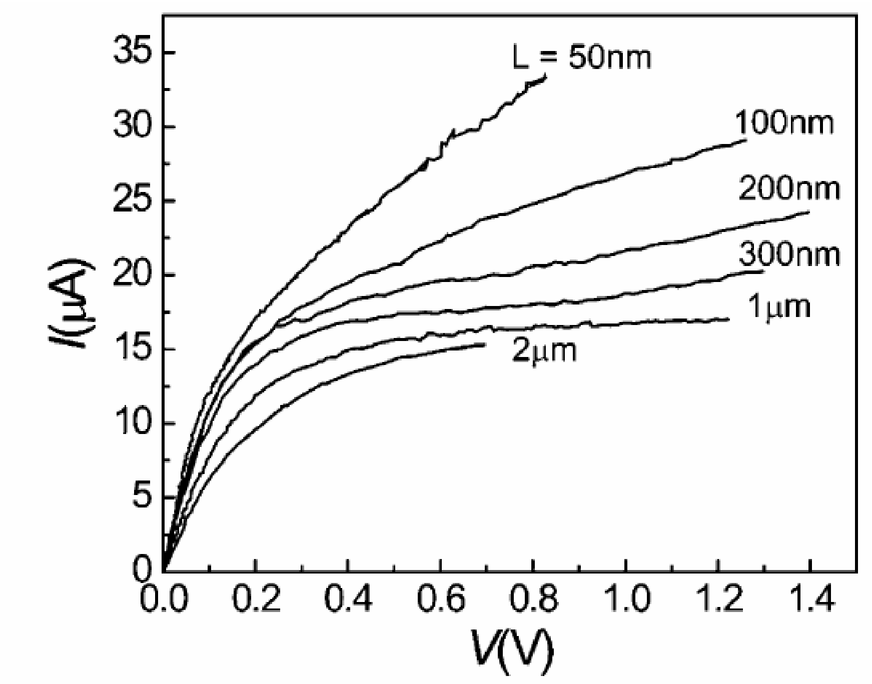

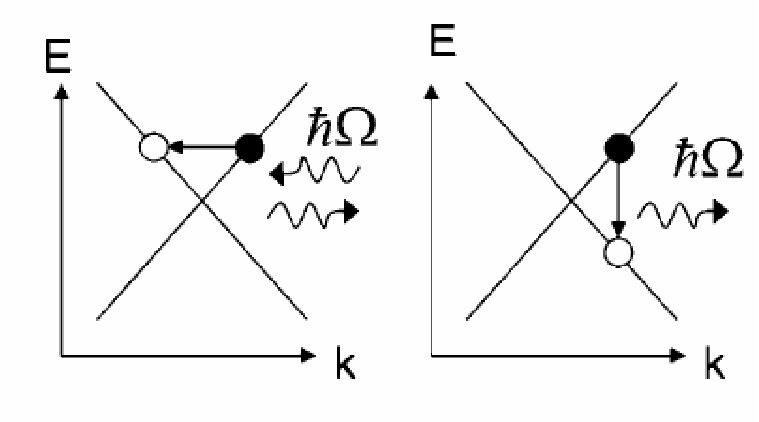

(a)

(b)

(a) Low bias, acoustic phonon scattering via absorption and emission

(b) high bias, longitudinal optical phonon (LO) emission when eV>hΩ (LO phonon energy), resulting in strong back scattering.

saturation current I~20-25μA in long channels.

Room T, metallic tube

$$R = \left(\frac{h}{4e^2}\right)\left(\frac{L}{l}\right)$$

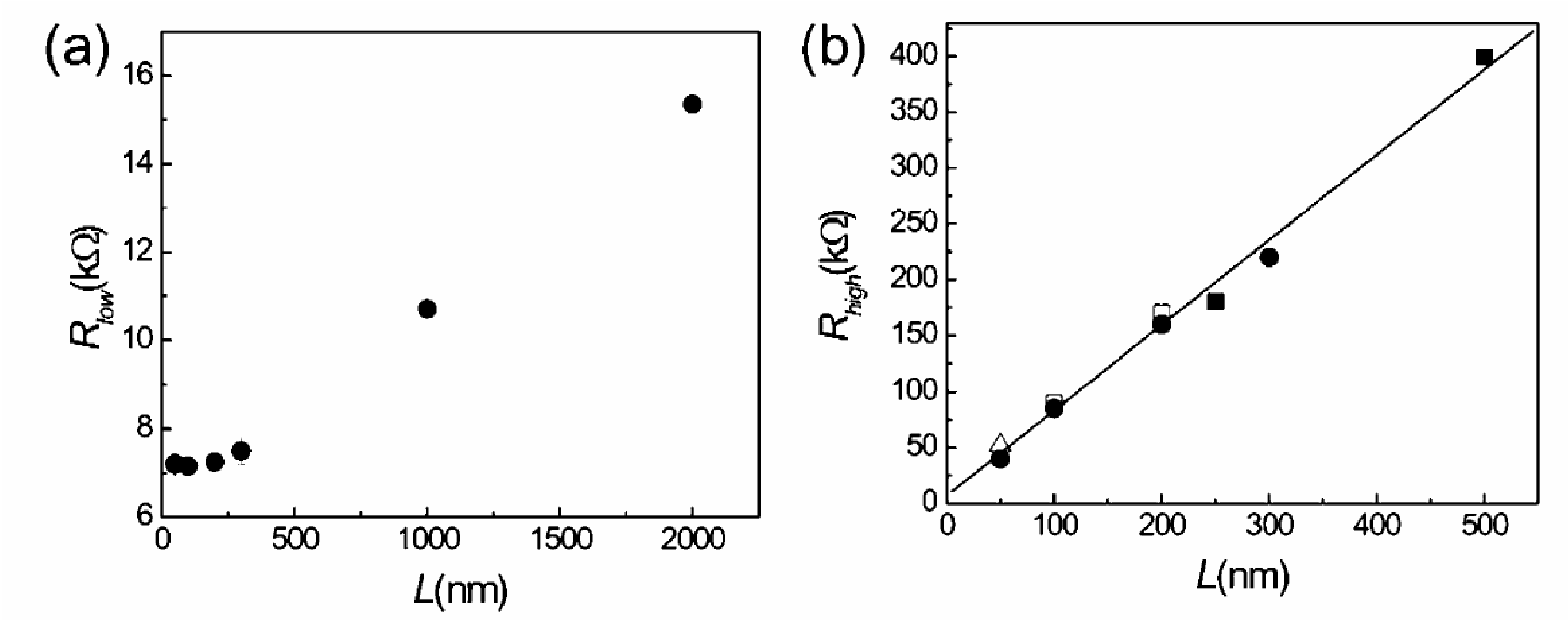

Low bias

l~1.6μm

High bias

l~15nm

Ballistic transport can be achieved for L<l, hard to achieve at large biases

Semiconducting tubes

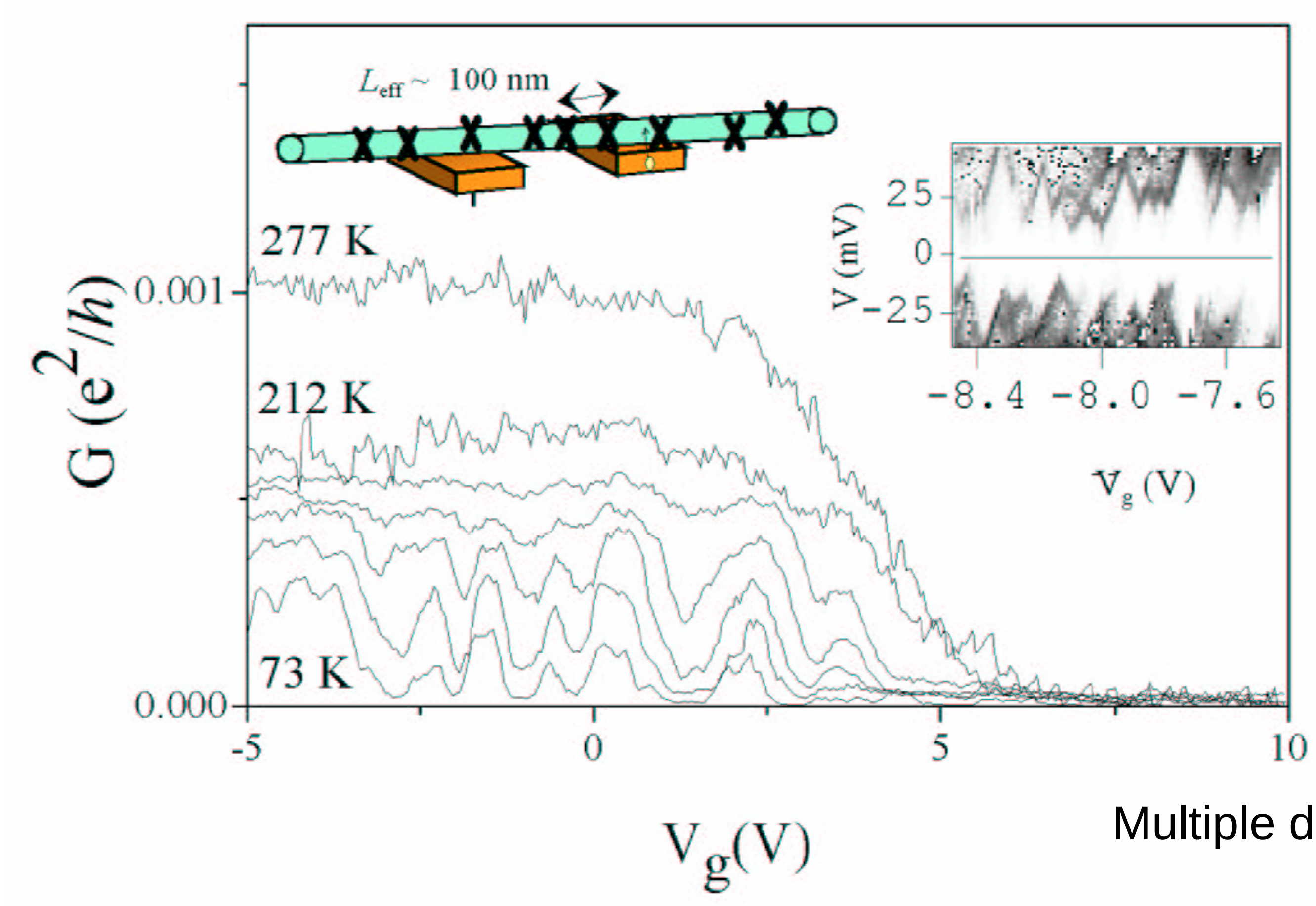

Multiple dot behavior

Disorder scattering, effective spacing ~100nm
(metallic tubes more immune to disorder scattering due to unique band structure)

Semiconducting tubes – Contact doping

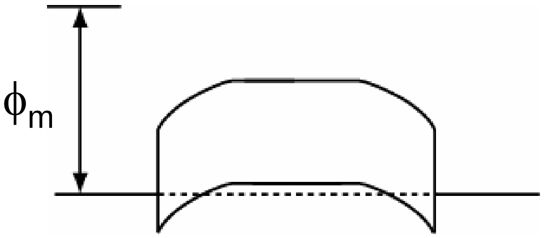

p-type

Most cases

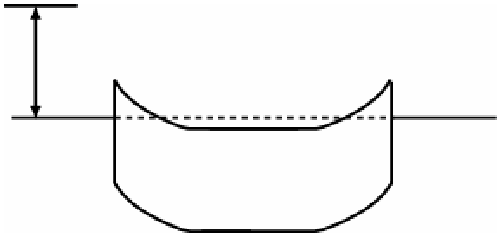

n-type

Contact doping:
Au, Pd contacted nanotubes show p-type behavior
Al contacted nanotubes show n-type behavior

Chemical doping with K atoms to form n-tubes, not well understood

Semiconducting tubes – Schottky barriers

Martel, PRL, **87**, 256805 (2001)

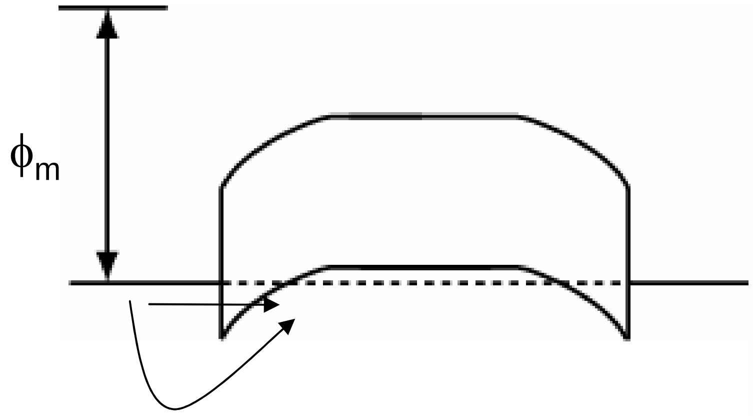

Thermal emission

$$j \propto \exp\left(-\frac{e\phi_B}{kT}\right)\left[\exp\left(\frac{eV}{kT}\right)-1\right]$$

S.M.Sze, p261

Tunneling emission

$$j \propto \exp(-2kd)$$

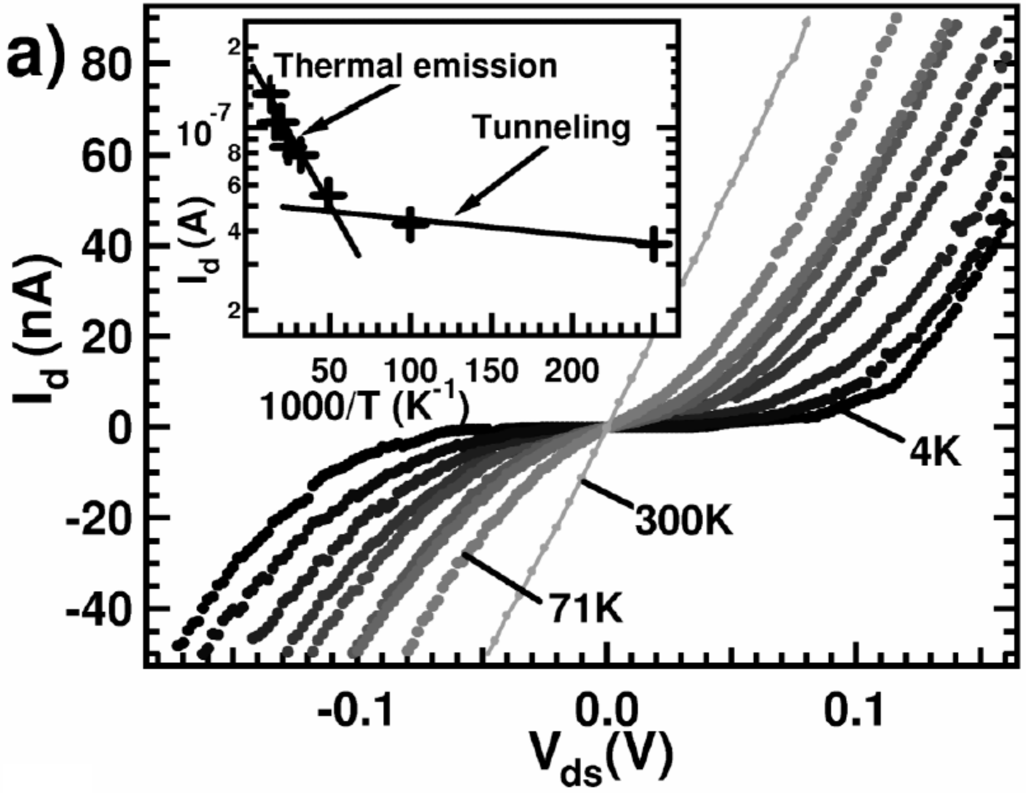

Device (all semiconducting CNT devices before 2003) performance dominated by Schottky barriers, rather than intrinsic tube properties.

Optical emission from CNT FET

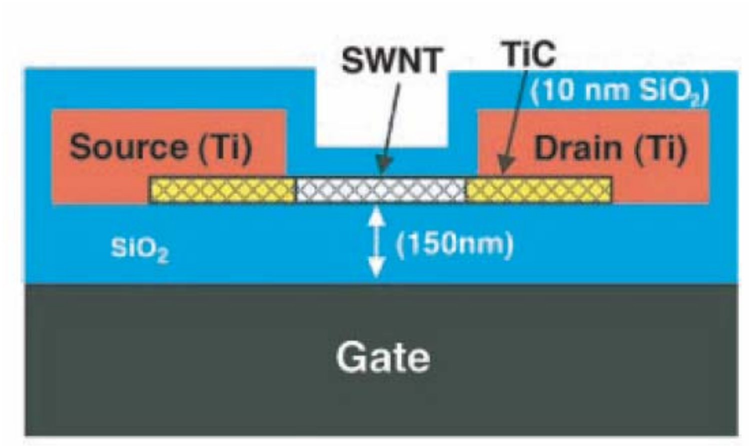

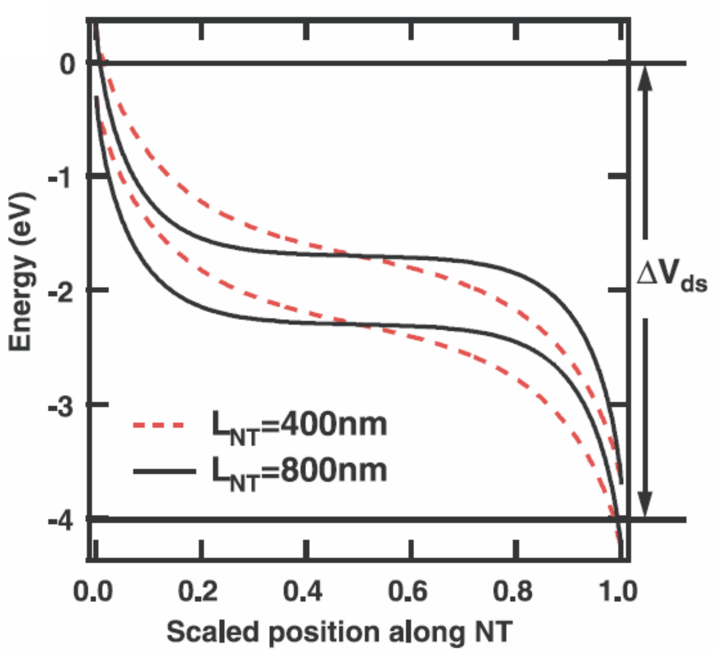

Ambipolar injection of carriers at large biases

Misewich, Science, **300**, 783 (2003)

Optical emission from CNT FET

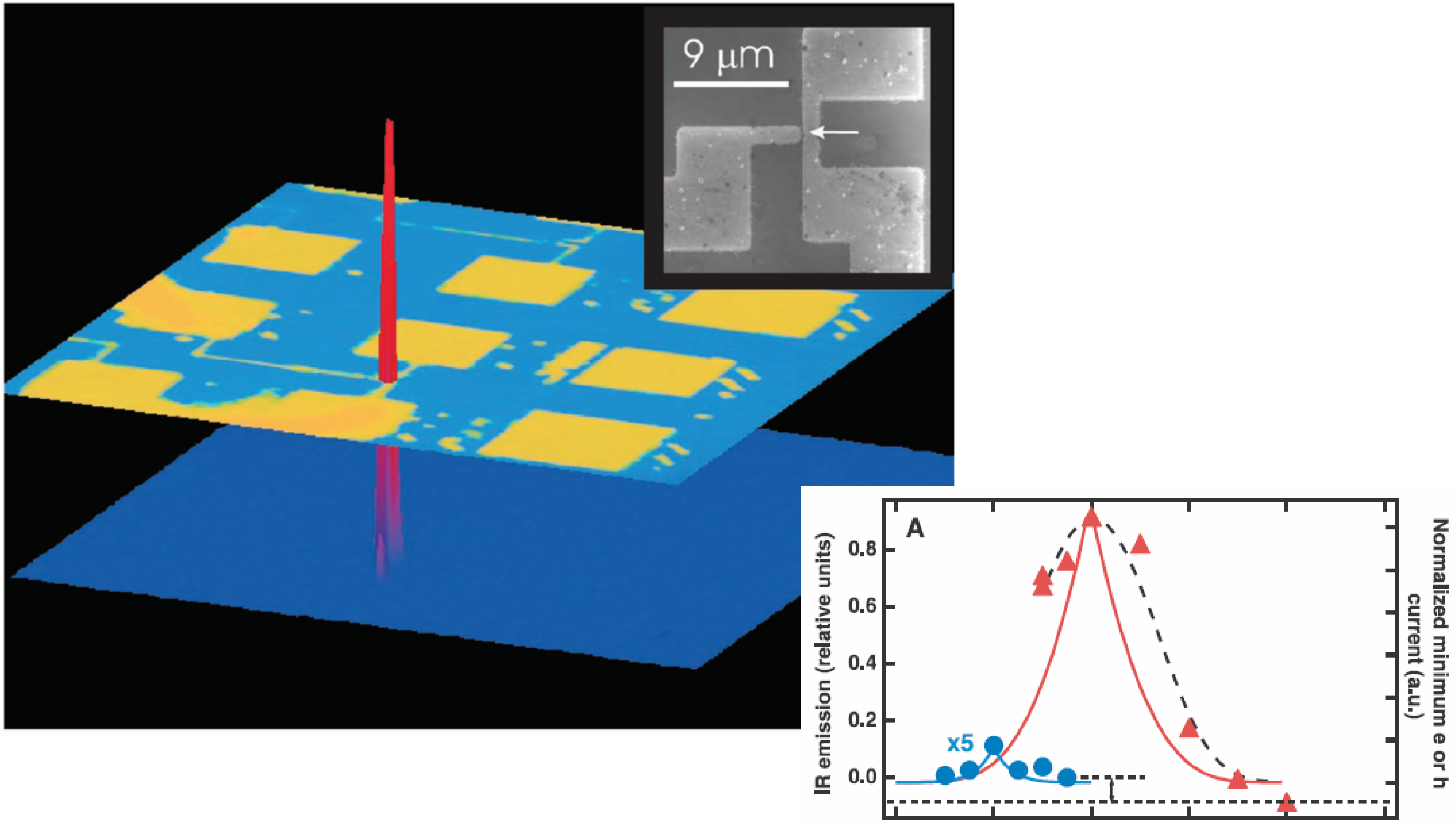

Misewich, Science, **300**, 783 (2003)

Semiconducting tubes, Ohmic contacts

Javey, Nature, **424**, 6949 (2003).

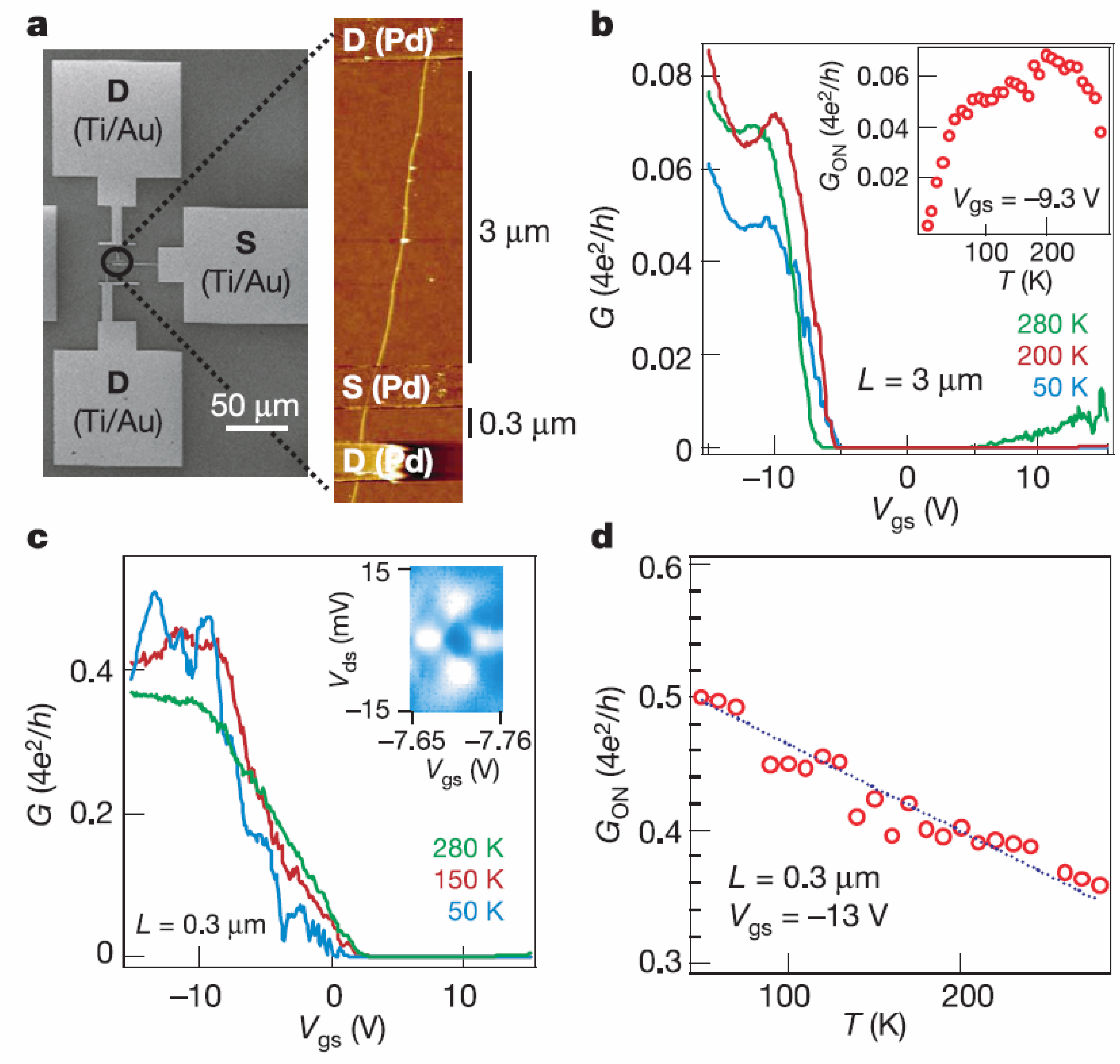

Semiconducting tubes, Ohmic contacts

Javey, Nature, **424**, 6949 (2003).

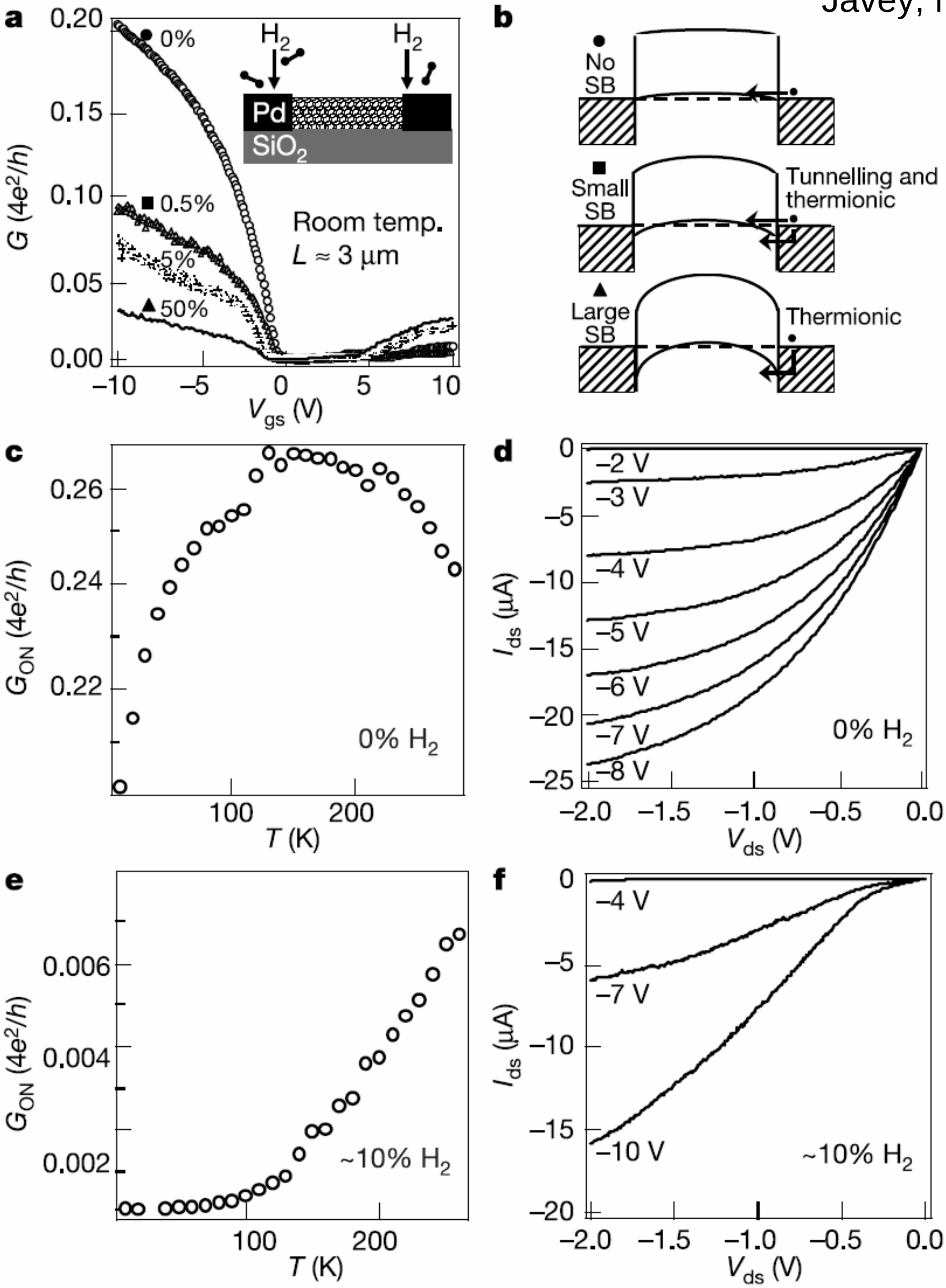

Semiconducting tubes, Ohmic contacts

Javey, Nature, **424**, 6949 (2003).

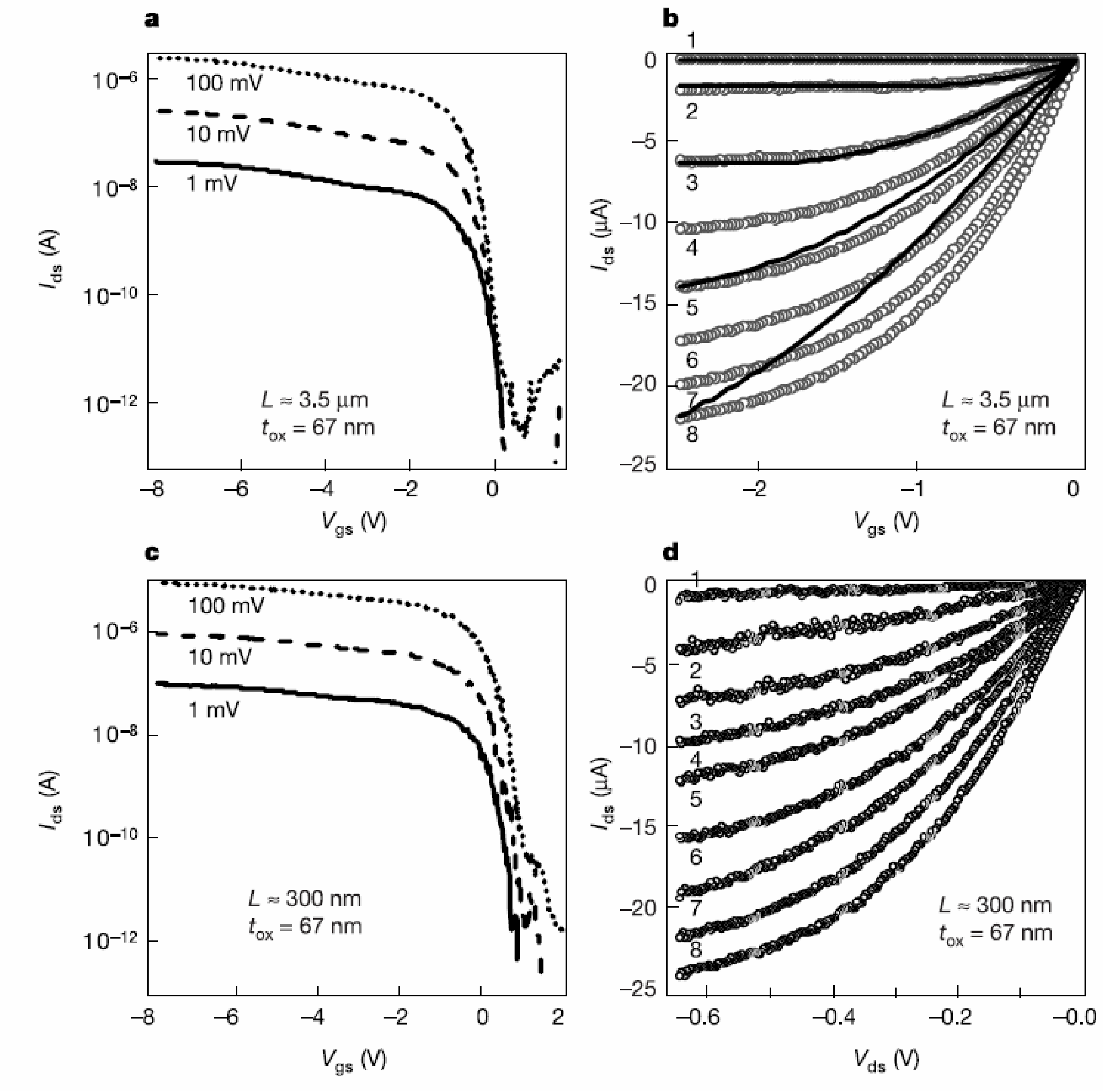

Self-aligned FET with high-k dielectrics

Javey, Nano Lett, **4**, 1319 (2004)

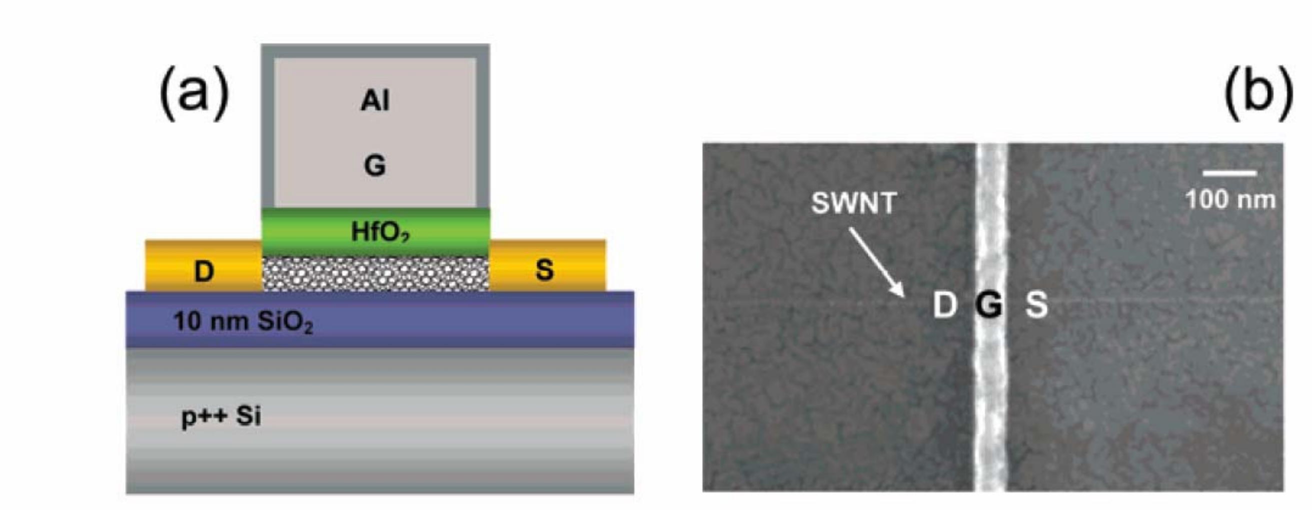

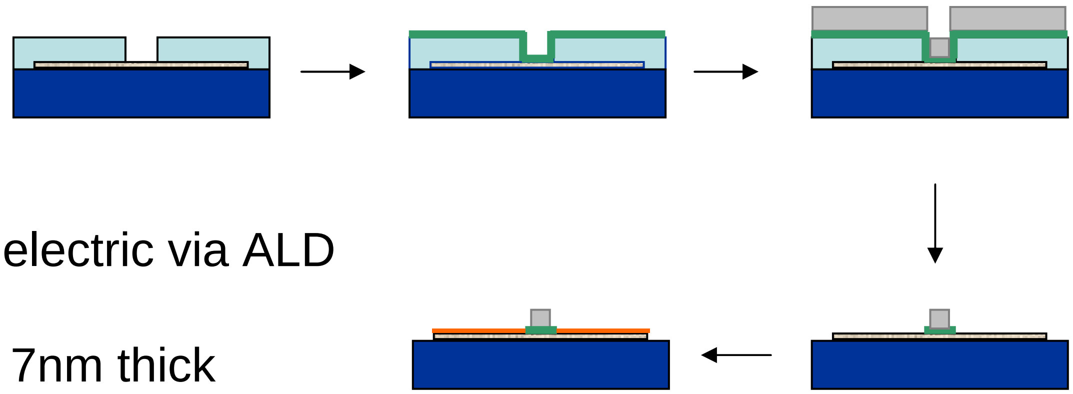
e-beam lithography

ALD

Al evaporation

Lift-off

Pd evaporation

8nm thick HfO2 dielectric via ALD
Al top gate
Pd S/D electrode, 7nm thick
L~50nm

Self-aligned FET with high-k dielectrics

Javey, Nano Lett, **4**, 1319 (2004)

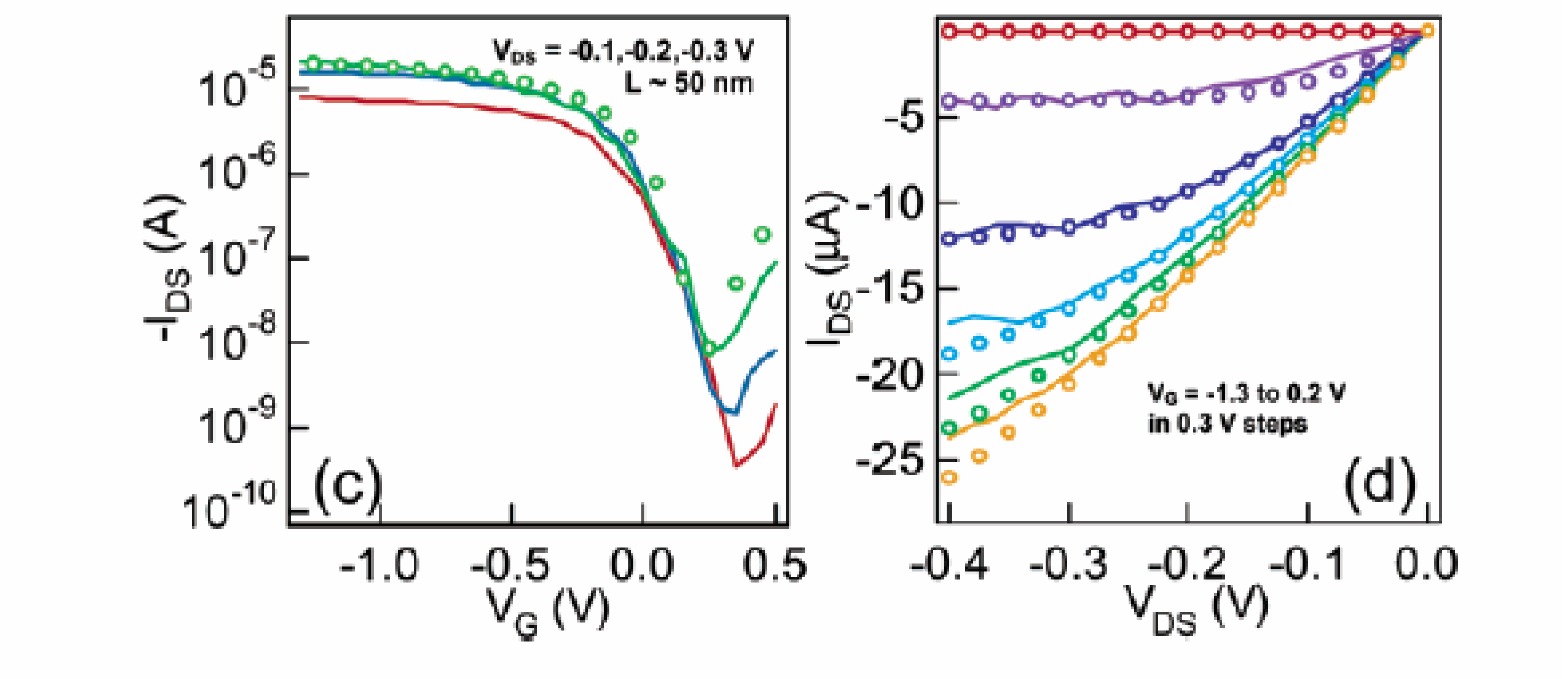

Best CNT device performance:

I_{on}~25μA

Peak G_m~30μS

I_{on}/I_{off}~10^3

S~110mV

Data agrees with ballistic FET simulation

Semiconducting tubes, different diameters

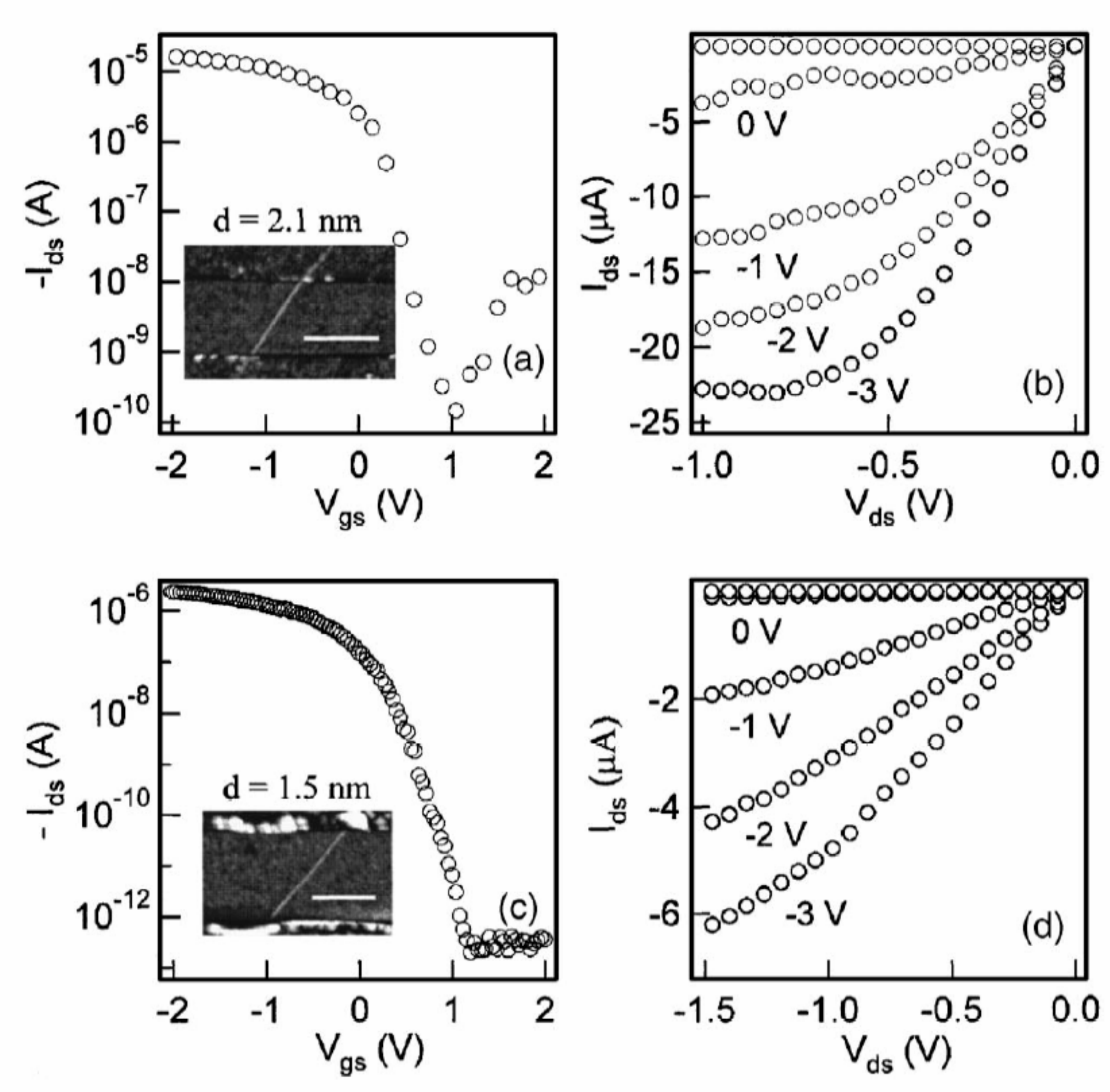

Ambipolar behavior

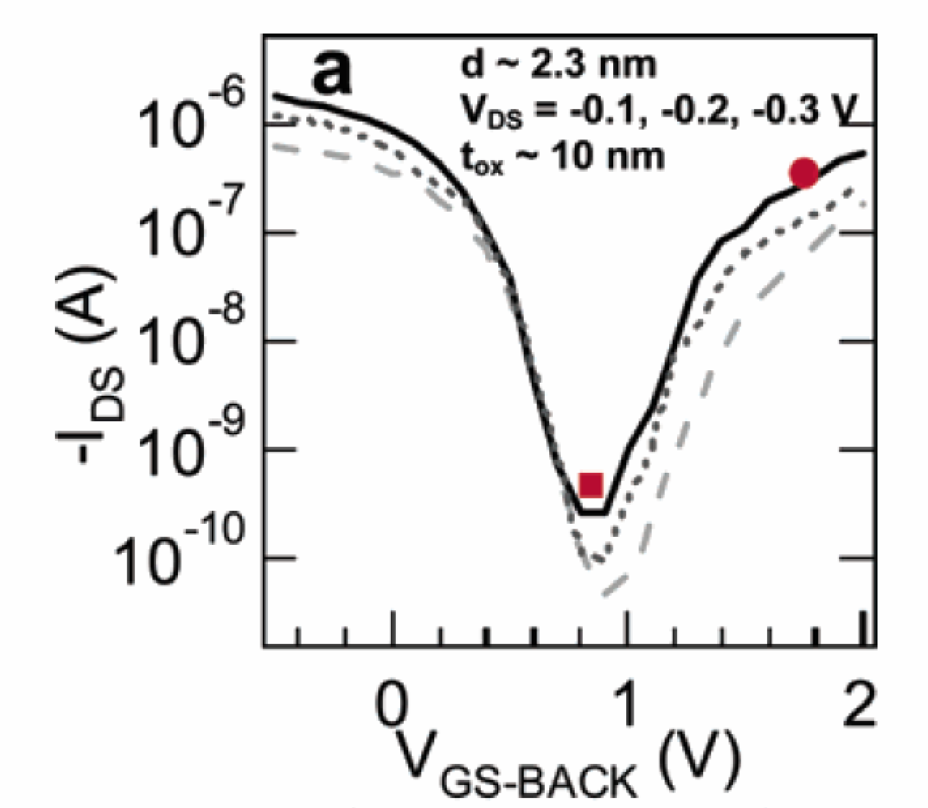

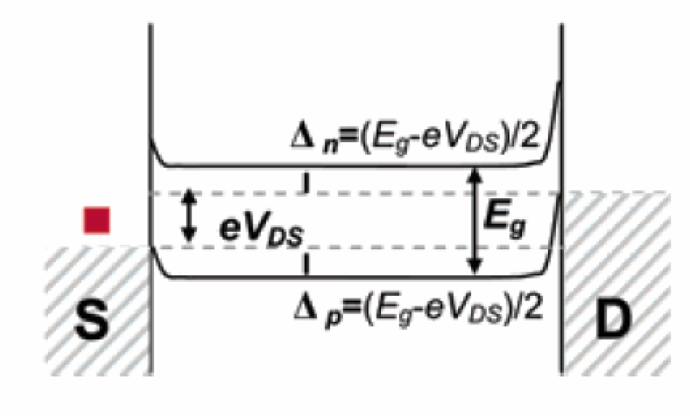

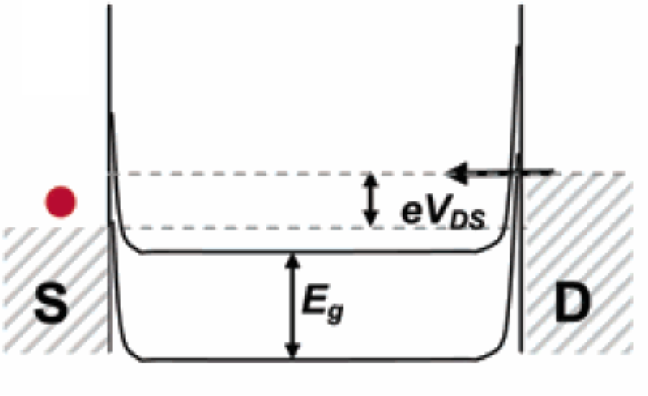

I_{off} upturn due to electron transport at very large gate voltage

Semiconducting tubes, different diameters

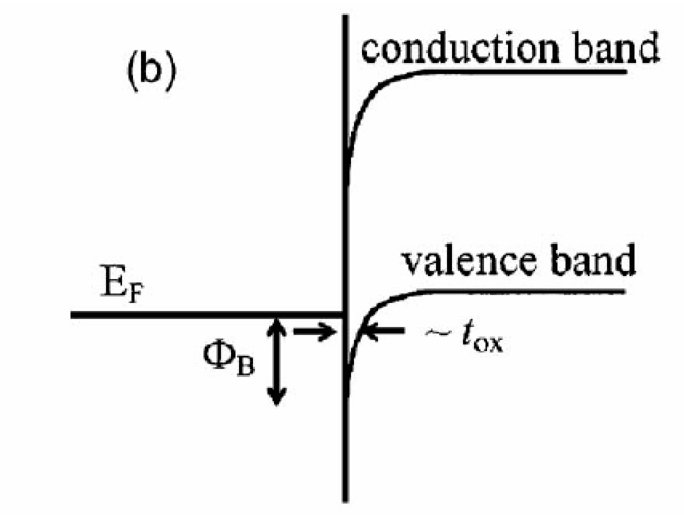

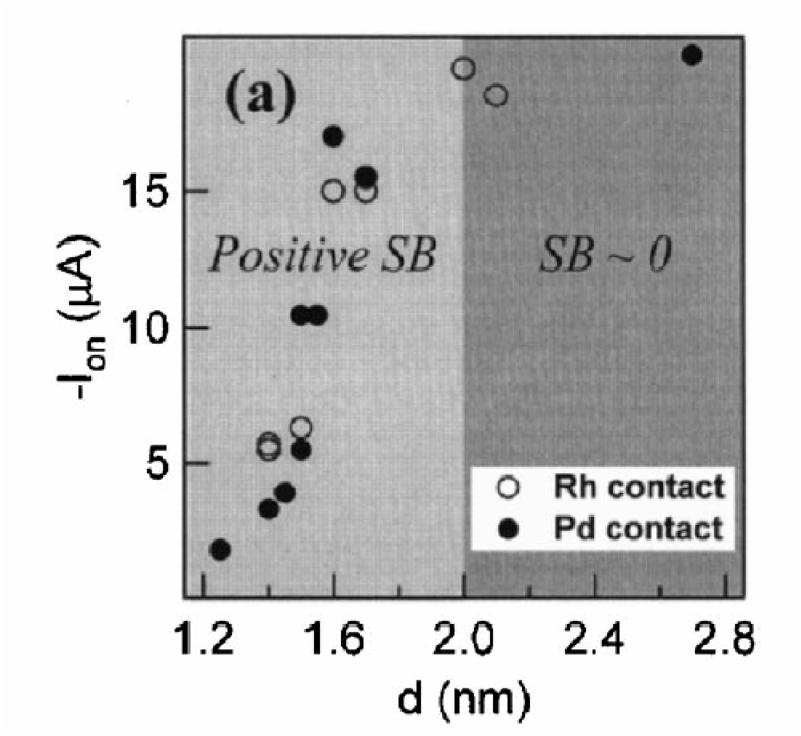

Difficult to make Ohmic contacts to tubes with diameter < 2nm

Summary of nanotube devices

Metallic tubes:

Easier to contact (no bandgap)
At small bias, long mean free path (>1μm) even at room T
At large bias, LO phonon scattering, l~15 nm
Can serve as interconnect, I>10^9A/cm^2

Semiconducting tubes:

Pd, for p-type, Al for n-type
More prone to defect and phonon scattering
At room T, l~500nm at small bias, l~15nm at large bias
Excellent mobility (μ~10^3-10^4cm^2/Vs), G_m, I_{on}

Challenges:

Separation of metallic/semiconductor tubes
Device yield
Fabrication of complementary devices
Large scale integration and assembly

Theory of ballistic FET

Modeled on analysis by Mark Lundstrom (ECE, Purdue). Unless otherwise indicated, all images are his.

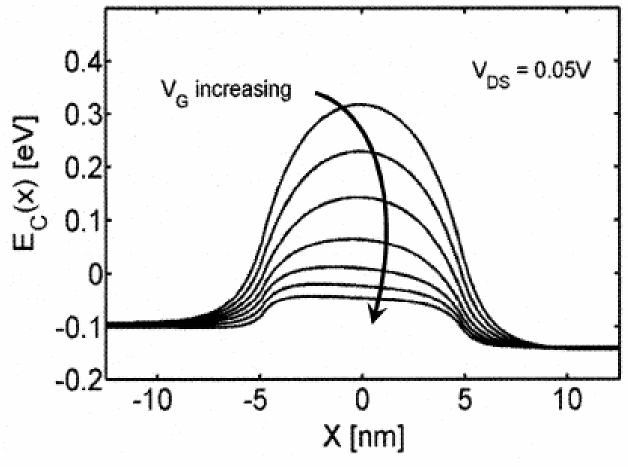

(a)

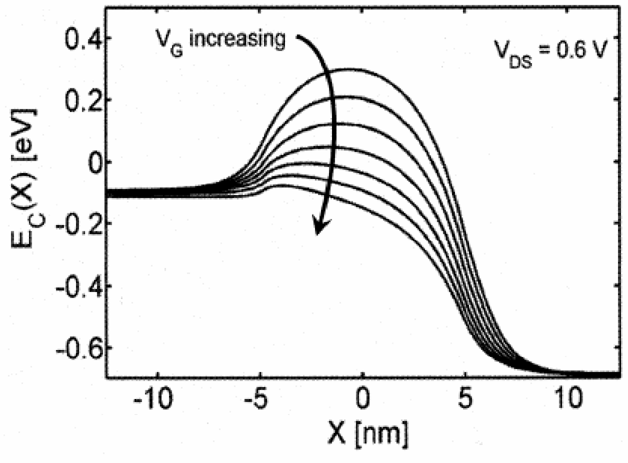

(b)

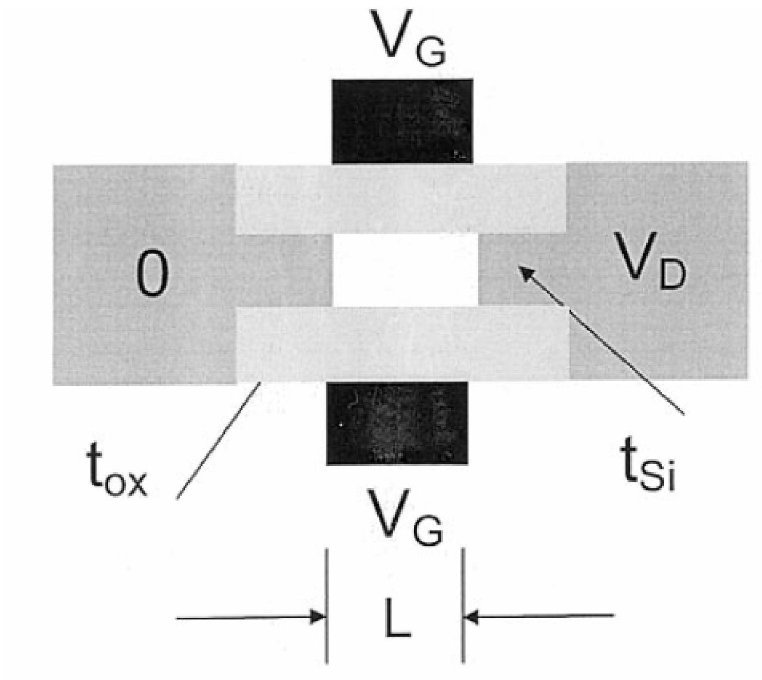

Potential profile inside channel

Nonequilibrium velocity (momentum) distributions

Remember our Landauer formula discussions? We worked in 1d and considered the chemical potential at different places along a device:

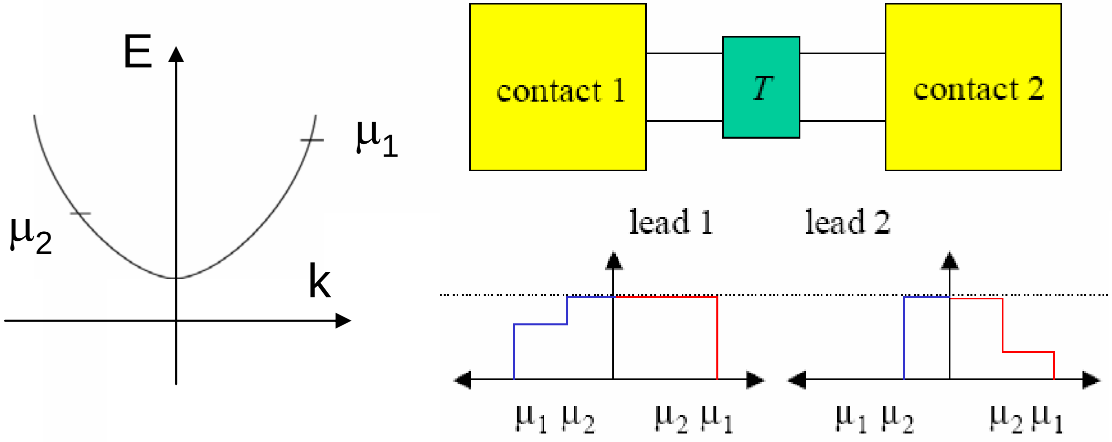

Can do same thing here, but plot velocity (momentum) distributions as a function of position:

Landauer formula: $G = \frac{2e^2}{h}\sum_i T_i$

Distribution function

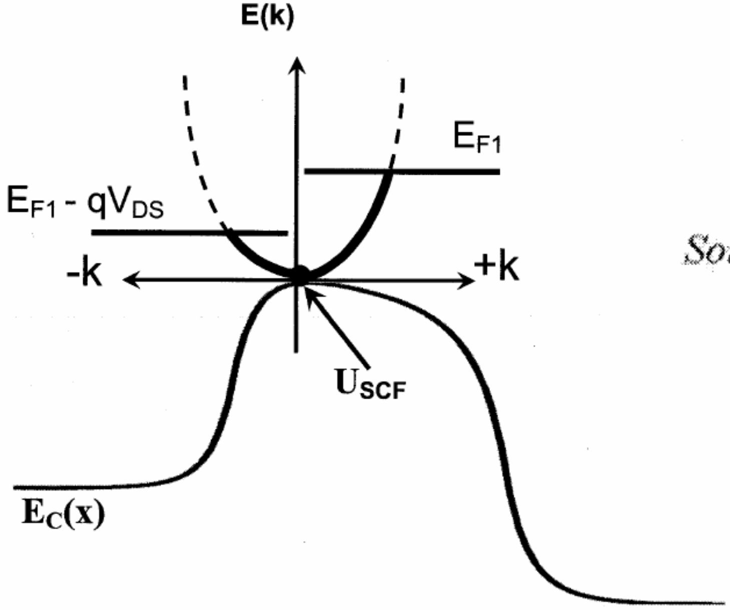

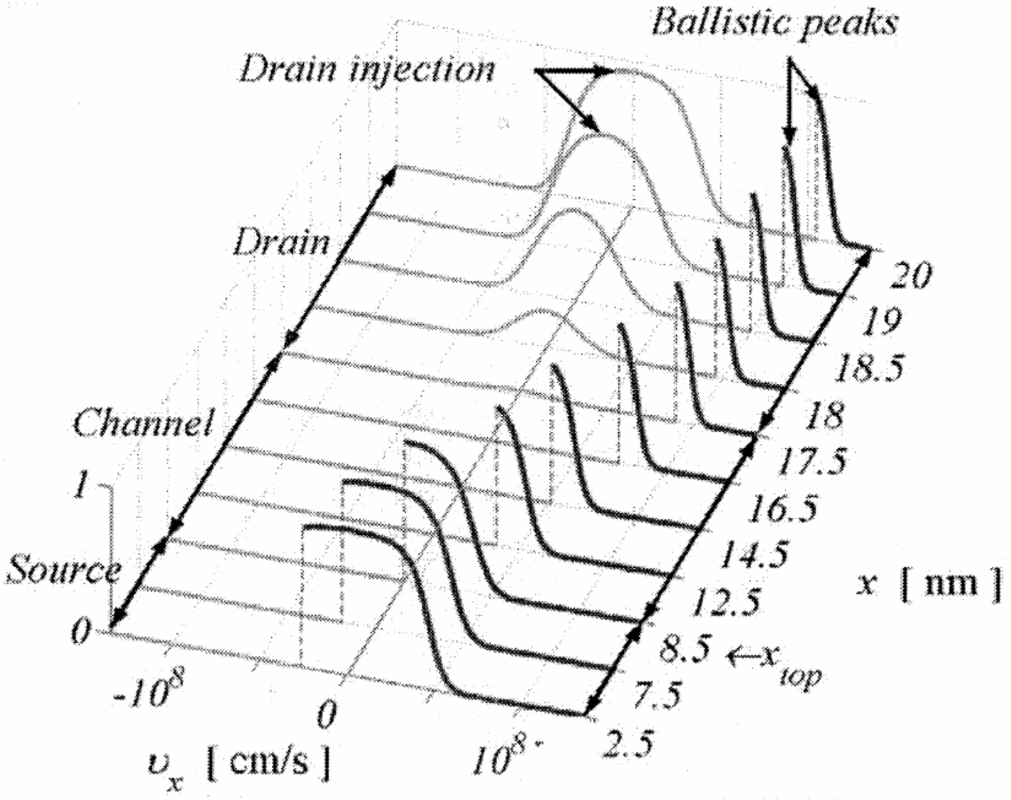

Current constant throughout the channel -> calculate I at the top of the barrier

$T \sim 0$, degenerate case, linear regime $E_F \gg k_B T$

$$I_D = I^+(E_F) - I^-(E_F - eV_D)$$

$$I^+(E_F) - I^-(E_F - eV_D) \approx \left(\frac{\partial I^+}{\partial E_F}\right) eV_D$$

Assuming hard transverse walls, transverse modes spaced by (π/W) in k space,

$$I^+(E_F) = eW \frac{\hbar k_F^3}{3\pi^2 m_*} = eW \frac{(2m_* E_F)^{3/2}}{3m_* \pi^2 \hbar^2}$$

Result: $$I_D = \left(\frac{2e^2}{h}\right)\left(\frac{Wk_F}{\pi}\right) V_D$$

→ This is the Landauer expression, with M, the number of channels, given by

$$M = \frac{k_F}{\pi / W}$$

→ $$\boxed{I_D = M\left(\frac{2e^2}{h}\right) V_D}$$

$T \sim 0$, degenerate case, “saturated” regime

If transistor is “on” all the way, current is just I^+ :

$$I^+(E_F) = eW\,\frac{\hbar k_F^3}{3\pi^2 m_*}$$

For 2d gas (one vert. subband, many transverse modes), all the *right*-moving carriers must be due to gate:

$$n_{2d}^{tot} = \frac{k_F^2}{4\pi} = \frac{C_x(V_G - V_T)}{e}$$

Plugging in,

$$\boxed{I_{Dsat} = WC_x(V_G - V_T)\left[\left(\frac{8\hbar}{3m_*}\right)\sqrt{C_x(V_G - V_T)/q\pi}\right]}$$

T~0

Saturation happens when V_D pulls right contact Fermi level below bottom of conduction band.

This happens here:

$$\boxed{V_{Dsat} = \left(\frac{C_x}{e^2(\nu_{2d}/2)}\right)(V_G - V_T)}$$

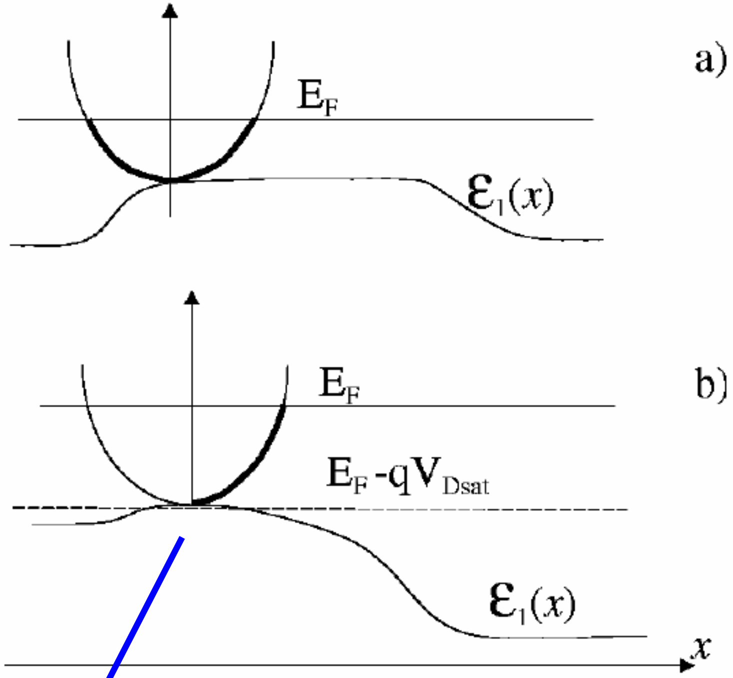

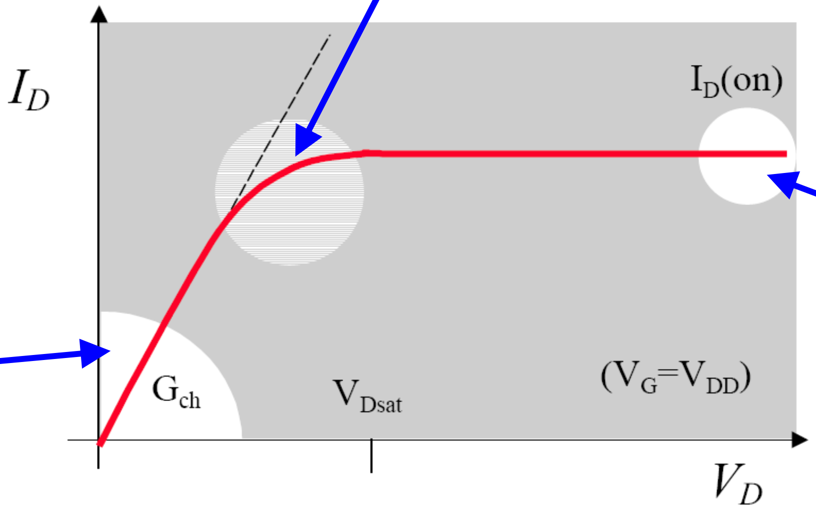

Linear region: conductance quantization

$$I_{D(on)} = I^+$$

T >> 0 case, nondegenerate carriers $k_BT>>E_F$

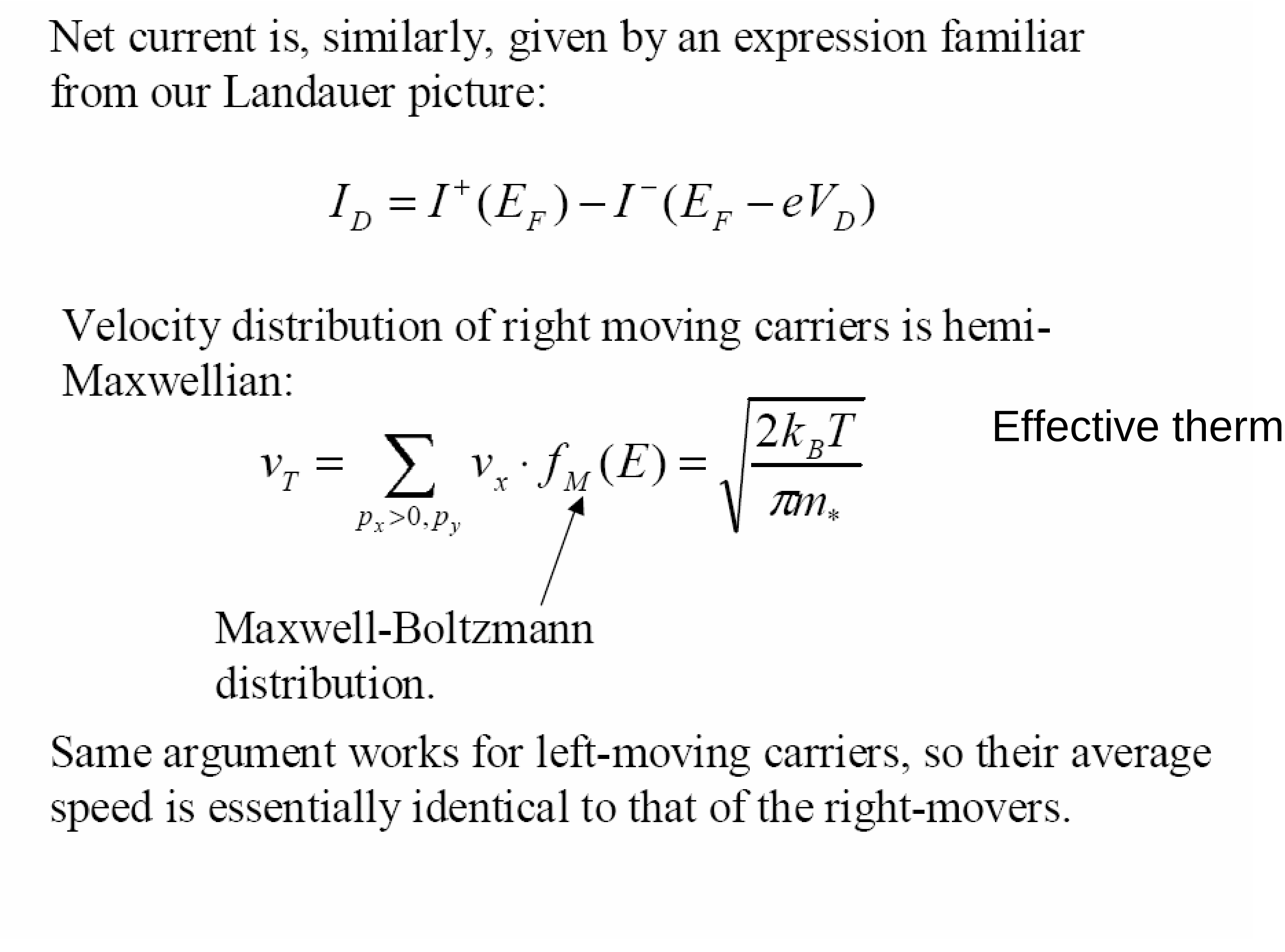

Net current is, similarly, given by an expression familiar from our Landauer picture:

$$I_D = I^+(E_F) - I^-(E_F - eV_D)$$

Velocity distribution of right moving carriers is hemi-Maxwellian:

$$v_T = \sum_{p_x>0,\,p_y} v_x \cdot f_M(E) = \sqrt{\frac{2k_BT}{\pi m_*}}$$

Maxwell-Boltzmann distribution.

Same argument works for left-moving carriers, so their average speed is essentially identical to that of the right-movers.

Effective thermal velocity

T >> 0 case, nondegenerate carriers

Resulting current density:

$$I_D / W = e n_{2d}^{+}(0) v_T - e n_{2d}^{-}(0) v_T$$

$$I_D / W = e n_{2d}^{tot} v_T \frac{(1 - n_{2d}^{+}(0) / n_{2d}^{-}(0))}{(1 + n_{2d}^{+}(0) / n_{2d}^{-}(0))}$$

Ahh, but we can figure out the ratio $n_{2\mathrm{d}}^{+}/n_{2\mathrm{d}}^{-}$:

$$n_{2d}^{+} = \left(\frac{N_{2d}}{2}\right) \exp\left(\frac{E_F - E}{k_B T}\right)$$

$$n_{2d}^{-} = \left(\frac{N_{2d}}{2}\right) \exp\left(\frac{E_F - eV_D - E}{k_B T}\right)$$

where $N_{2d} = \left(\frac{m_*}{\pi\hbar^2}\right) k_B T$

Effective density of states

$$C_x (V_G - V_T) = n_{2d}^{tot}$$

T >> 0 case, nondegenerate carriers

Result for current density:

$$I_D / W = e n_{2d}^{tot} v_T \frac{(1 - n_{2d}^{+}(0)/n_{2d}^{-}(0))}{(1 + n_{2d}^{+}(0)/n_{2d}^{-}(0))} \longrightarrow I_D / W = e n_{2d}^{tot} v_T \frac{(1 - e^{-eV_D/k_B T})}{(1 + e^{-eV_D/k_B T})}$$

Plugging in our expression for carrier density in a "nice" FET gives:

$$\boxed{I_D = W C_x (V_G - V_T) v_T \frac{(1 - e^{-eV_D/k_B T})}{(1 + e^{-eV_D/k_B T})}}$$

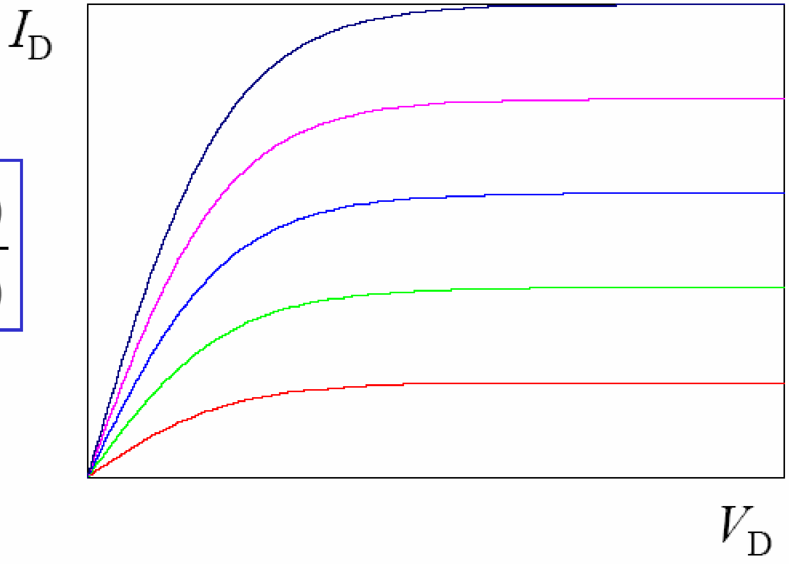

T >> 0 case, linear regime

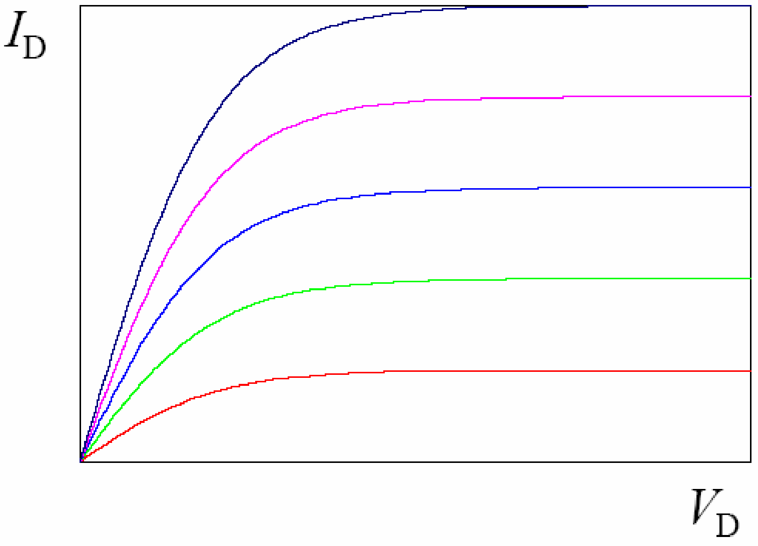

We can expand

$$I_D = WC_x(V_G - V_T)v_T \frac{(1 - e^{-eV_D/k_BT})}{(1 + e^{-eV_D/k_BT})}$$

for small eV_D/k_BT to find linear regime behavior:

$$\boxed{I_D \approx \left[WC_x(V_G - V_T)\frac{v_T}{2k_BT/e} \right] V_D}$$

So, channel conductance $G = WC_x(V_G - V_T)\frac{v_T}{2k_BT/e} = \frac{I_{Dsat}}{2k_BT/e}$

Regular MOSFET has $G = WC_x(V_G - V_T)\frac{\mu}{L}$

Since regular MOSFET can never be better than ballistic case,

$\rightarrow \frac{\mu}{L}\frac{2k_BT}{e} < v_T$ $\quad v_T = \sqrt{\frac{2k_BT}{\pi m^*}}$ Upper limit on mobility….

T >> 0 case, linear regime

$$G = WC_x(V_G - V_T)\frac{v_T}{2k_BT/e}$$

Note that channel conductance is *finite* even for ballistic case, as in Landauer picture.

Here, it’s a direct consequence of the thermionic emission model used here when examined at small bias.

Left-moving current down from right-moving current by $\exp(-eV_D/k_BT)$

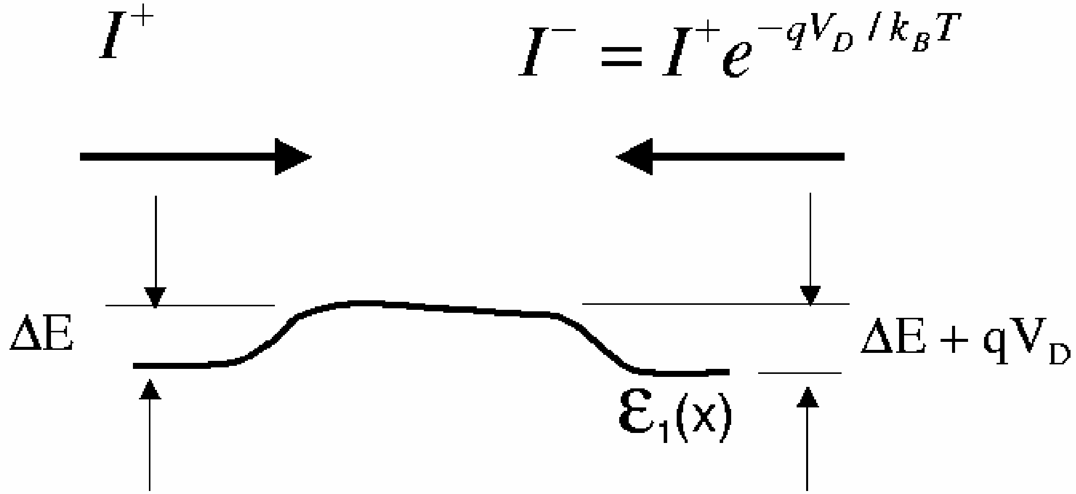

T >> 0 case, sturation regime

There is saturation at high V_D, because all current is determined by charge density at top of barrier, where effective velocity saturates out to the hemi-Maxwell mean velocity.

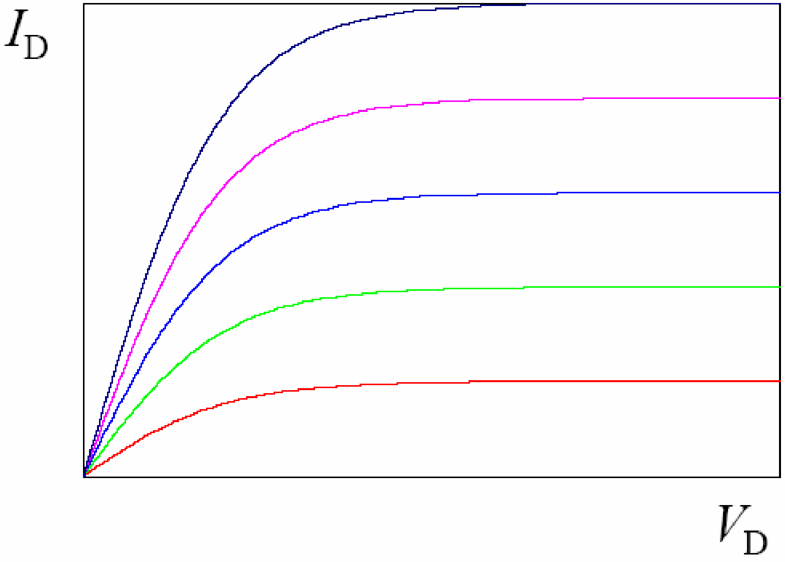

Unlike the standard MOSFET, V_{Dsat} is *independent* of V_G:

$$I_D = WC_x(V_G - V_T)v_T \frac{(1-e^{-eV_D/k_BT})}{(1+e^{-eV_D/k_BT})} \longrightarrow V_{Dsat} \approx \frac{2k_BT}{e}$$

For $V_D >> V_{dsat}$,

$$\boxed{I_{Dsat} = WC_x(V_G - V_T)v_T}$$

Ballistic FET compared to conventional MOSFET

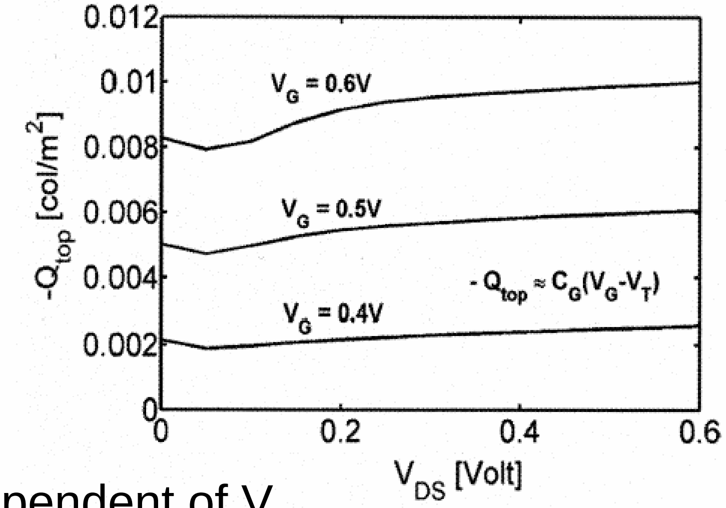

n independent of V_{DS}

(a)

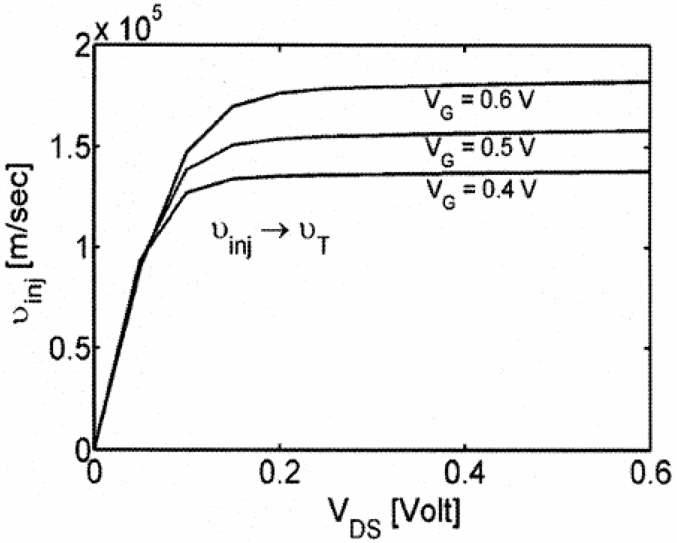

Velocity saturates to V_T

Determined by barrier near Source

MOSFET

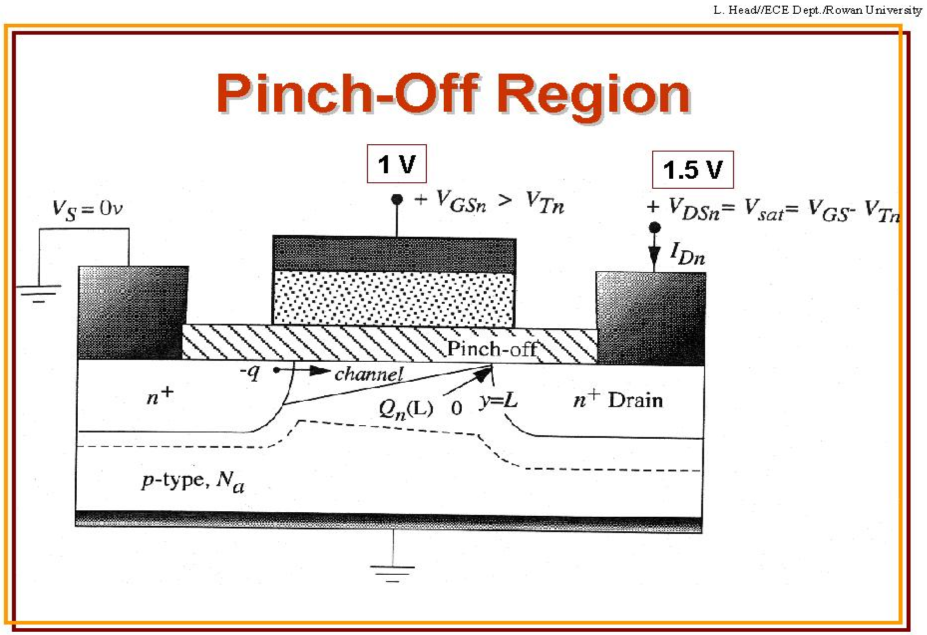
L. Head//ECE Dept./Rowan University

Pinch-Off Region

Pinch-off near Drain

n->0

Electric field and $v\uparrow$ as Vg$\uparrow$

IEEE Transactions on Electron Devices (50) 9, September 2003.

General finite temperature results:

Defining the general Fermi-Dirac integral of order *s* as:

$$F_s(\eta) \equiv \int_0^\infty \frac{x^s dx}{\exp(x-\eta)-1}$$

and the normalized drain voltage: $U_D \equiv V_D / (k_B T / e)$

and the normalized Fermi energy: $\eta_F \equiv (E_F - \varepsilon_1) / k_B T$

we find:

$$I_D = eWC_x (V_G - V_T) \widetilde{v}_T \left[\frac{1 - F_{1/2}(\eta_F - U_D) / F_{1/2}(\eta_F)}{1 + F_0(\eta_F - U_D) / F_0(\eta_F)} \right]$$

where:

$$\widetilde{v}_T = \sqrt{\frac{2k_B T}{\pi m_*}} \frac{F_{1/2}(\eta_F)}{F_0(\eta_F)}$$

General finite temperature results:

Saturation regime: $I_{Dsat} = eWC_x(V_G - V_T)\tilde{v}_T$

Linear regime: $I_D = \left[WC_x(V_G - V_T)\dfrac{\tilde{v}_T}{2(k_B T / e)} \right] \left(\dfrac{F_{-1/2}(\eta_F)}{F_0(\eta_F)} \right) V_D$

Summary of Ballistic FETs

- Quantum confinement effects strongly affect transmission in ballistic nanoscale MOSFETs.

- Ignoring source-drain tunneling, velocity saturation happens near source at high bias, Determined by v_F or v_T

- For good electrostatic design, result is current determined just by V_G and source properties.

- Can derive analytic expressions under these conditions for nondegenerate, degenerate, or arbitrary T conditions.

- Conductance near zero source-drain bias is still finite, even when device is ballistic.

- A melding of classical MOSFET theory and a Landauer way of thinking about such problems….